LA-11277-MS

Accurate, Wide-Range Uranium Enrichment Measurements by Gamma-Ray Spectroscopy

I. Characterization of Enrichment Standards

II. Demonstration of Enrichment Measurement Capability

Los Alamos

Los Alamos National Laboratory is operated by the University of California for the United States Department of Energy under contract W-7405-ENG-36.

Prepared by Kathleen Atencio, Stand By, Lucretia M. Henson, HRD-Secretarial Resources, and Jo Ann Barnes, Group N-1

This work was supported by the US Department of Energy, Office of Safeguards and Security.

An Affirmative Action/Equal Opportunity Employer

This report was prepared as an account of work sponsored by an agency of the United States Government. Neither the United States Government nor any agency thereof, nor any of their employees, makes any warranty, express or implied, or assumes any legal liability or responsibility for the accuracy, completeness, or usefulness of any information, apparatus, product, or process disclosed, or represents that its use would not infringe privately owned rights. Reference herein to any specific commercial product, process, or service by trade name, trademark, manufacturer, or otherwise, does not necessarily constitute or imply its endorsement, recommendation, or favoring by the United States Government or any agency thereof. The views and opinions of authors expressed herein do not necessarily state or reflect those of the United States Government or any agency thereof.

LA-11277-MS

UC-15
Issued: September 1988

Accurate, Wide-Range Uranium Enrichment Measurements by Gamma-Ray Spectroscopy

I. Characterization of Enrichment Standards
II. Demonstration of Enrichment Measurement Capability

J. L. Parker
M. Brooks*

*Undergraduate student at Los Alamos.

Los Alamos National Laboratory
Los Alamos, New Mexico 87545

CLASSIFICATION

CONTENTS

ABSTRACT 1

I. CHARACTERIZATION OF ENRICHMENT STANDARDS 2

A. The Problem 2

B. Characterization Procedures 2

1. Selection and Mechanical Measurements of Cans 2

2. Repackaging and Sampling 5

3. Analysis Work Performed 6

a. Analyses at LANL's Group CHM-1 6

b. Analyses at NBL 7

C. Results of Analyses 7

1. Results of Mass Spectrometric Measurements . 7

2. Results of Analyses for Uranium Fractions . 20

3. Results of Emission Spectrometric Analyses . 22

D. Comparison with Gamma-Ray Measurements and Designation of Primary and Secondary Standards . 24

II. DEMONSTRATION OF ENRICHMENT MEASUREMENT CAPABILITY . 26

A. Experimental Procedures 26

1. Review of the Measurement Physics and the Required Corrections 26

2. Apparatus and Data Acquisition Procedures . 34

3. Data Analysis Procedures 36

B. Measurement Results 46

1. Comparative Measurements on NBS SRM-969 . . 47

2. Comparisons Between SRM-969 and Some LANL Standards 49

3. Comparison Among LANL Standards of $\leq$3% Enrichment 51

CONTENTS (cont)

4. Comparison Among LANL Standards of ≥10% Enrichment 53
5. Final Remarks on Precision and Accuracy . . 56

REFERENCES 58

APPENDIX. ALL LANL AND NBL VALUES OF ATOM PERCENT ^{235}U . 60

ACCURATE, WIDE-RANGE URANIUM ENRICHMENT MEASUREMENTS BY GAMMA-RAY SPECTROSCOPY

I. Characterization of Enrichment Standards

II. Demonstration of Enrichment Measurement Capability

by

J. L. Parker and M. Brooks

ABSTRACT

Section I describes the repackaging and recharacterization of 19 approximately 1-kg lots of uranium oxides, with enrichments (^{235}U at.%) ranging from 0.7 to 91 at.%, for use primarily as working standards in gamma-ray enrichment measurements. The results of all characterization analyses are given. We found a surprising degree of isotopic inhomogeneity in about half the lots of oxide. We divided them into primary and secondary groups according to the degree of homogeneity and confidence in the average measured enrichments. For both groups, we give tables for best-value ^{235}U atom fractions, nominal values of other isotopes, uranium fractions, oxide mass, uranium mass, ^{235}U mass, approximate impurity levels, and container composition and thickness (both lid and bottom). The recharacterized materials are now valuable for studying other nondestructive assay measurements as well as for gamma-ray enrichment measurements.

Section II describes demonstration gamma-ray enrichment measurements on the Los Alamos National Laboratory standards and on the National Bureau of Standards (NBS) certified enrichment reference standards (NBS SRM-969). We consider in some detail both the theoretical and experimental considerations of doing accurate gamma-ray measurement of uranium enrichment, including particularly the extraction of the net area of spectral full-energy peaks, correction for deadtime and pileup losses, correction for the chemical composition of the measured materials, and correction for the attenuation in containers. We conclude that with proper procedures and careful work, gamma-ray enrichment measurements based on a minimum set of standards (perhaps only one of high enrichment) can be made over the whole range of enrichments $\geq 0.7\%$ with biases of $\leq 0.1\%$.

I. CHARACTERIZATION OF ENRICHMENT STANDARDS

A. The Problem

There currently exists no set of certified reference materials for the gamma-ray spectrometric determination of uranium enrichment (^{235}U atom fraction) that covers a wide range of enrichment. The only set of certified standards now available is that jointly issued by the National Bureau of Standards (NBS) and the Central Bureau for Nuclear Measurements (CBNM). This set (NBS SRM-969/CBNM EC NRM-171) covers only the range from 0.3 to 4.5 at.% of ^{235}U. Because of this lack of certified standards and the desirability of investigating the possible accuracy of gamma-ray enrichment determinations over a wide range of enrichment, Los Alamos National Laboratory's (LANL) Safeguards Assay Group (N-1) in early 1985 undertook the repackaging and recharacterization, for use as working standards, of 19 approximately 1-kg lots of uranium oxide. These materials included 12 enrichments between normal (0.7 at.%) and 91 at.%. Table I gives the identifications, nominal enrichments, and nominal chemical compositions.

The 19 lots of oxide had been acquired over a period of about 15 years from several sources. They were packaged in poorly characterized cans, and in most cases there had been only routine quality determinations of isotopic ratios and uranium fractions based on a single small sample. Previous gamma-ray measurements had already demonstrated that there were inconsistencies of up to 2% relative among the then-available enrichment values. We thought that repackaging and recharacterizing these oxides would provide in a reasonably economical way a valuable set of working standards to use in investigating the limits of gamma-ray enrichment measurement. Such a set of standards would also be potentially useful for studying the accuracy of the necessary corrections for deadtime and pileup, which are important in all measurements based on high-resolution gamma-ray spectroscopy, as well as for some applications in neutron-based nondestructive assay (NDA).

B. Characterization Procedures

1. Selection and Mechanical Measurements of Cans. The 19 lots of oxide were contained in standard tinned steel food cans containing ~1 ℓ. Unfortunately, the bottoms of the cans were corrugated, making it difficult to

TABLE I

IDENTIFICATION, NOMINAL ENRICHMENT,
AND NOMINAL COMPOSITIONS OF LANL OXIDES

Standard ID	Nominal Enrichment (% ^{235}U)	Nominal Composition
UISO-91	91	U_3O_8
UISO-66	66	U_3O_8
UISO-52	52	U_3O_8
UISO-38	38	U_3O_8
UISO-27	27	U_3O_8
UISO-17	17	U_3O_8
UISO-13	13	U_3O_8
UISO-12	12	U_3O_8
A1-323-1	10	U_3O_8
A1-324-1	10	U_3O_8
A1-324-2	10	U_3O_8
A1-1126-1	3	UO_2
A1-1126-2	3	UO_2
A1-1125-1	2	UO_2
A1-1125-2	2	UO_2
A1-1127-1	0.7	UO_2
A1-1127-2	0.7	UO_2
A1-409	0.7	U_3O_8
A1-408-2	0.7	U_3O_8

accurately calculate the attenuation of gamma rays passing through them, thus making a change of container nearly mandatory. Eventually, a flat-bottomed, tinned-steel can with a slip lid was selected. Figure 1 is a mechanical schematic of the can with dimensions in inches. Table II gives the pertinent information in metric units. The thicknesses of both bottoms and lids were carefully measured by the LANL inspection shop. Five measurements were made with precisions of 0.0001 in. (0.0025 mm) at the center and the ends of the arms of a cross centered on either bottom or lid, the arms on the cross being 2.00 in. long from end to end (not from center). In addition, the maximum and minimum thicknesses along the two arms of the cross were recorded. Although

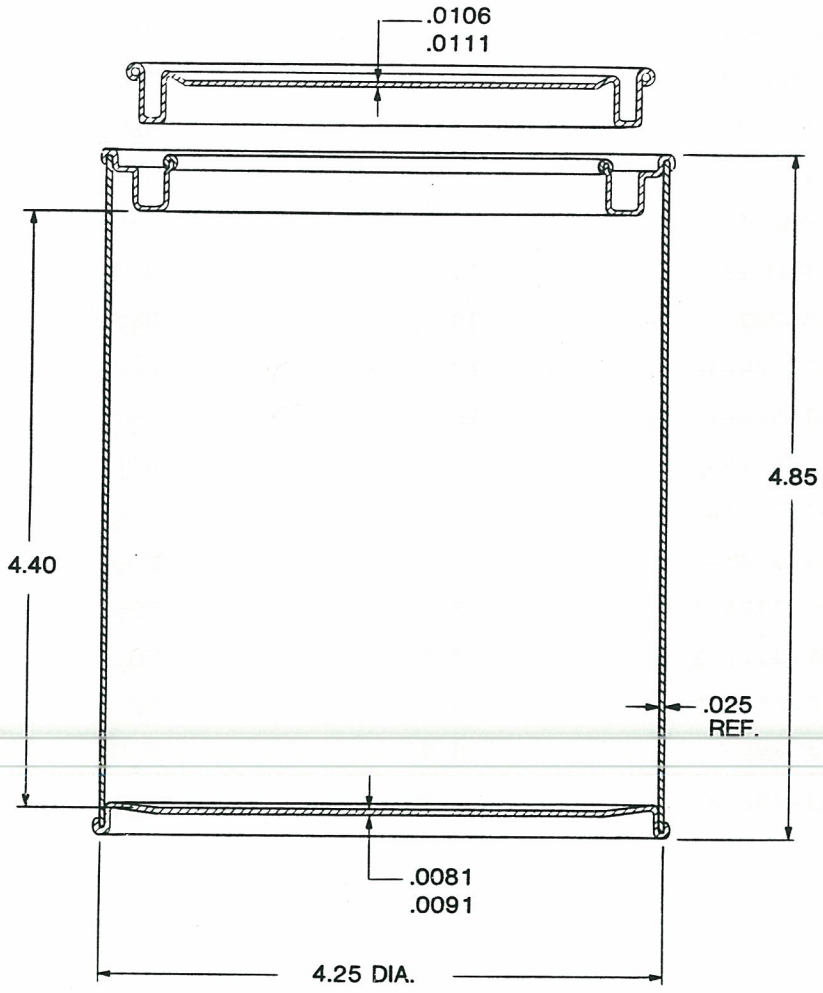

Fig. 1. Mechanical shematic of the can used for repackaging the 19 lots of uranium oxide. All dimensions on shematic are in inches.

TABLE II

DIMENSIONS AND COMPOSITION OF ENRICHMENT STANDARD CANS

Range of bottom thickness	0.206-0.231 mm
Range of top thickness	0.269-0.282 mm
Inside diameter	108.0 mm
Nominal wall thickness	0.64 mm
Approximate depth	123.0 mm
Approximate volume	1.0 ℓ
Composition:	
Fe	>99.0%
Mn, Si, C	Variable, few tenths % each
Density	7.86 g/cm^3
Sn plating, each side	~0.00075 mm

the average thickness of the bottoms varied by 0.001 in. (0.025 mm), the thickness of no individual one varied by more than ±0.0001 in. from its average. The thicknesses of individual lids varied within the same tolerance while the average thicknesses varied only by 0.0005 in. As seen in Table II, the composition is such that computations of estimated transmissions through the bottoms and lids may be based, with very little error, on an assumption of a pure iron composition with a density of 7.86 g/cm^3. The variability of the minor constituents is so great that there is no point in trying to include it in any computations. The thickness of tin is <1% of the iron and sufficiently variable that there is again no point in trying to compensate for it in computations of transmission. After the new containers were filled, the lids were firmly positioned and fastened with four spots of high-temperature solder and then sealed with a bead of silicon-based rubber sealant.

2. Repackaging and Sampling. During the repackaging procedure, six ~2-g samples (labeled A, B, C, D, E, and F) were removed from each lot of oxide for characterization. Efforts were made to obtain the samples from throughout the volume of each lot. After the oxides were transferred into the carefully weighed empty cans they were weighed again to obtain the net weight of the

contents. The oxides were not blended or remixed as part of the repackaging procedure because there was considerable reason to believe that the oxides were isotopically homogeneous beyond the possibility of obvious improvement. There was also doubt that any available blender could be cleaned sufficiently between uses to eliminate the possibility of contaminating the various lots of oxides with residues left from previous lots. In retrospect, it might well have been wise to attempt blending the materials in spite of the difficulties, for isotopic inhomogeneity beyond anything remotely expected (among small samples from 30 to 50 mg) was found in a majority of the lots of oxide, as described in detail in Sec. I.C.1.

Of the six samples from each lot of oxide, we submitted three (A, B, and C) to LANL's Analytical Chemistry Group (CHM-1) for characterization analyses. Two samples (D and E) were submitted to the Department of Energy's New Brunswick Laboratory (NBL) for similar analyses, and one sample (F) was put into archival storage for possible future analyses.

3. Analysis Work Performed. As mentioned above, characterization analyses were performed at both LANL and NBL.

a. Analyses at LANL's Group CHM-1. The most important analysis for enrichment standards is obviously the isotopic distribution. Accordingly, each 2 g sample (A, B, and C) was divided, a 30 to 50 mg subsample from each portion dissolved, and one or two mass spectrometric determinations of the isotopic fractions were made on each dissolution. A second analysis for a given dissolution was made only when there was evidence of isotopic inconsistency among the six subsamples from a given lot.

The uranium fraction (g U/g UO_x) is of secondary importance in enrichment measurements, as explained in detail in Sec. II.A.1, but it is obviously necessary in determining the total grams of uranium in the lots of oxide. Accordingly, Group CHM-1 did gravimetric analyses on each of the 57 samples from the 19 lots of oxide to determine the mass fraction of uranium in sample.

The impurities in the oxides were thought to be at concentrations so low that they would not influence enrichment measurements at a level of more than a few hundredths of a percent. To confirm that assumption, semiquantitative emission spectroscopic analyses were done on one sample from each lot. It was fortunate that the information sought here was of the least importance because

the expense of the emission spectroscopic analyses was greater than either the mass spectrometric work (which was least expensive) or the gravimetric analyses.

b. Analyses at NBL. The isotopic distribution being of prime importance, NBL also divided its two samples (D and E) and made dissolutions of about 30 mg from each subsample. In every case, two independent mass spectrometric determinations of isotopic distribution were made from each dissolution. NBL thus made duplicate isotopic analyses for four separate samples from each lot of uranium oxide.

To determine the uranium mass fractions with best accuracy, NBL did Davies and Gray titration analyses on each of the 38 samples submitted. No emission spectrometric analyses were done at NBL because it was felt that the usefulness of the information to be obtained was not worth the cost of the effort.

C. Results of Analyses

1. Results of Mass Spectrometric Measurements. The immediate and disturbing conclusion on examining the results submitted by both laboratories was that a large fraction of the 19 lots of uranium oxide were not as isotopically homogeneous as had been thought. Both laboratories found variations in isotopic distributions among subsamples that were far greater than the precision of the mass spectrometers used. Table III presents the averages of the ^{235}U atomic fractions (expressed in percent) found by LANL and NBL along with the percent relative standard deviation (RSD) computed from the measured values. For NBL, the number of measured values was eight in nearly every case. For LANL, the number was six or more depending upon the sample and the apparent variation found within the first six determinations. Inasmuch as the number of values is small in all cases, the values of RSD have themselves a large uncertainly and they really give only a measure of the scatter of the measured values, which as commented above is in many cases much greater than expected. All the results going into the averages of Table III are given as reported by both laboratories in the Appendix. The last column of Table III gives the difference of NBL and LANL averages as a percentage of the average of LANL and NBL averages. It is seen that 9 of the 19 values are >0.1%, again far more

TABLE III

NBL AND LANL AVERAGES AND RSD(%)
OF MEASURED ATOM PERCENTS OF ^{235}U[9]

Standard ID	NBL		LANL		(NBL-LANL) • 100 / Average
	at.% ^{235}U[a]	RSD (%)	at.% ^{235}U	RSD (%)	
UISO-91	91.416	0.037	91.423	0.011	-0.007
UISO-66	66.313	0.031	66.322	0.022	-0.014
UISO-52	52.431	0.042	52.420	0.025	+0.021
UISO-38	37.834	0.048	37.870	0.116	-0.095
UISO-27	27.035	0.360	26.787	0.522	+0.920
UISO-17	17.430	0.098	17.489	0.126	-0.334
UISO-13	13.092	0.059	13.105	0.107	-0.094
UISO-12	11.911	0.044	12.008	0.833	-0.816
A1-323-1	10.240	0.268	10.250	0.410	-0.100
A1-324-1	10.201	0.096	10.204	0.069	-0.030
A1-324-2	10.200	0.047	10.201	0.039	-0.008
A1-1126-1	3.0665	0.049	3.073	0.293	-0.212
A1-1126-2	3.0647	0.140	3.065	0.228	-0.010
A1-1125-1	1.9612	0.046	1.962	0.102	-0.056
A1-1125-2	1.9606	0.031	1.964	0.255	-0.173
A1-1127-1	0.7253	0.110	0.7267	0.206	-0.193
A1-1127-2	0.7272	0.344	0.7270	0.138	+0.027
A1-408-2	0.7213	0.139	0.7225	0.138	-0.166
A1-409	0.7199	0.056	0.7211	0.139	-0.167

[a]For NBL, the averages and RSD(%) were based on eight measured values. For LANL, the averages and RSD(%) were based on six measured values.

than expected. Another striking feature of the list of differences is that only 3 of 19 are positive. If the two laboratories had prepared mass spectrometer filaments from the same solutions, that circumstance would be strong evidence of a bias between their measurements. However, that was not the case. The samples used by NBL and LANL were totally independent, and the evidence for relatively large variations in the ^{235}U atom fractions among samples of 30- to 50-mg size from the same lot of oxide is so compelling that it is impossible to ascribe the excess of negative differences between the LANL and NBL averages to biases between the two laboratories.

To make the scatter (or lack of it) among the results from a given lot of oxide more graphic, Figs. 2 through 20 present the results of all the ^{235}U determinations for each lot individually. In each figure, the percent deviations of the individual ^{235}U values from the average of all for a given lot of oxide are plotted on the vertical axis, and the sample identifications are given along the horizontal axis. As indicated on the figures, samples A, B, and C were analyzed at LANL and samples D and E at NBL. The results of the two subsamples from each major sample are widely spaced within the sample columns. Results from the same subsample dissolution are either one above the other

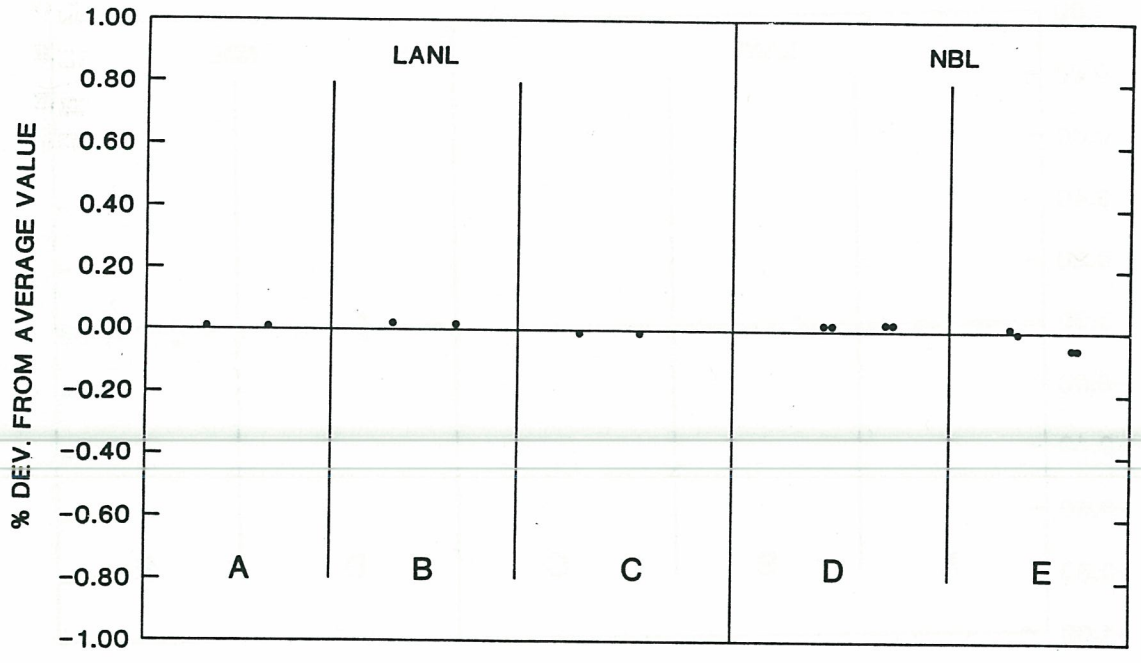

Fig. 2. Plot showing the scatter of the mass spectrometric values for the ^{235}U atom fractions in the samples from lot UISO-91 (~91.4 at.% ^{235}U).

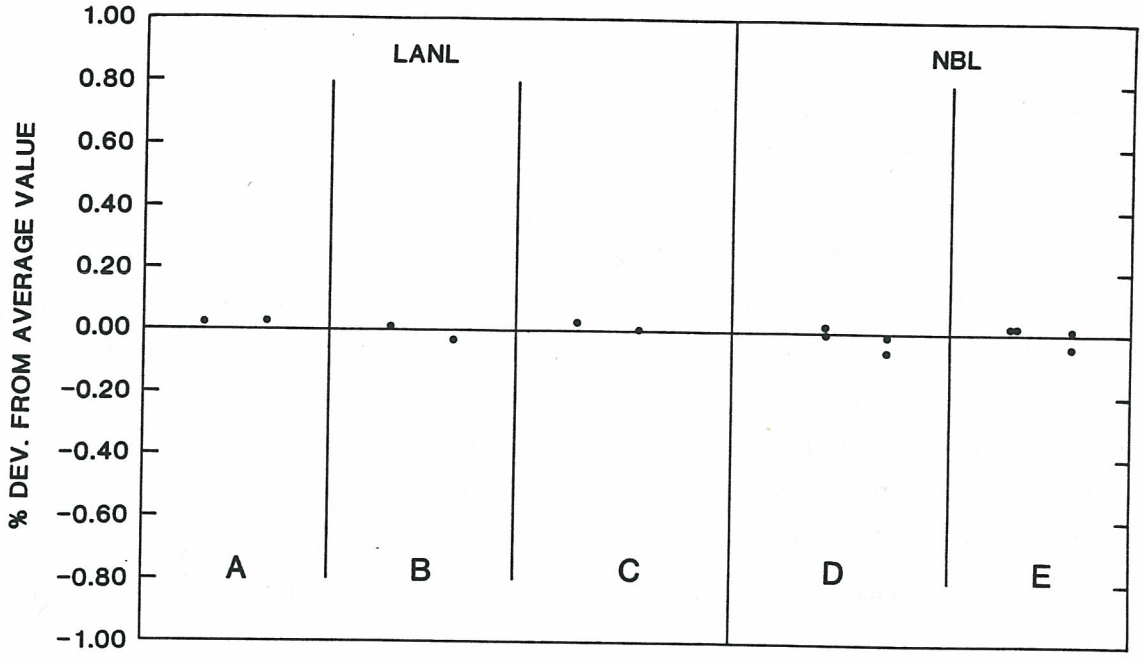

Fig. 3. Plot showing the scatter of the mass spectrometric values for the ^{235}U atom fractions in the samples from lot UISO-66 (~66.3 at.% ^{235}U).

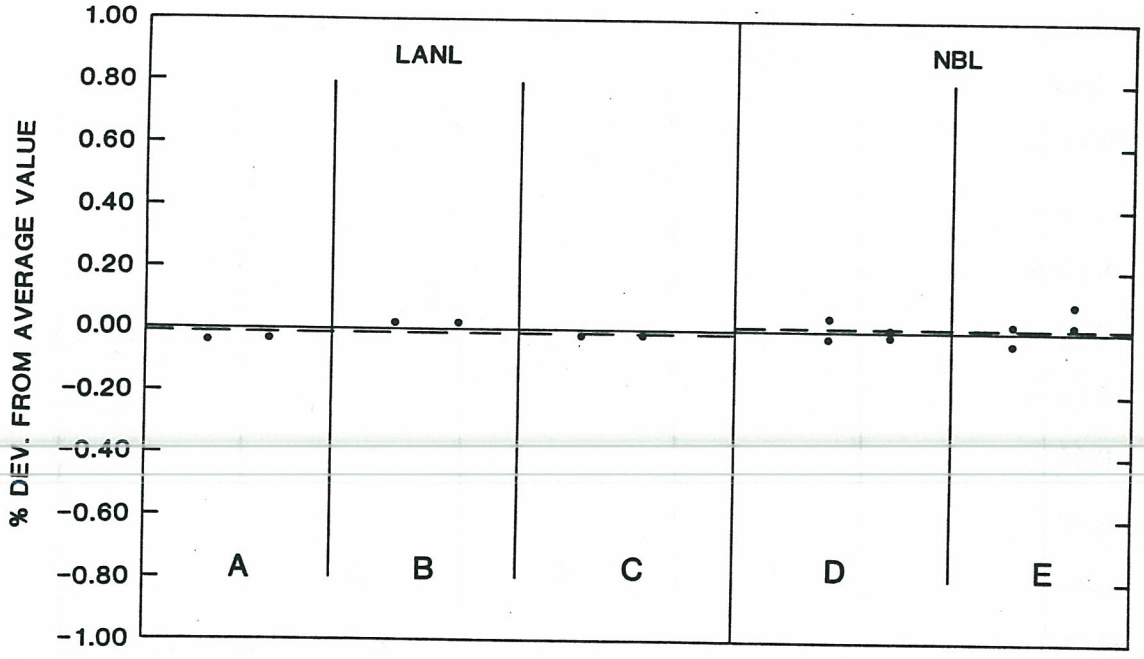

Fig. 4. Plot showing the scatter of the mass spectrometric values for the ^{235}U atom fractions in the samples from lot UISO-52 (~52.4 at.% ^{235}U).

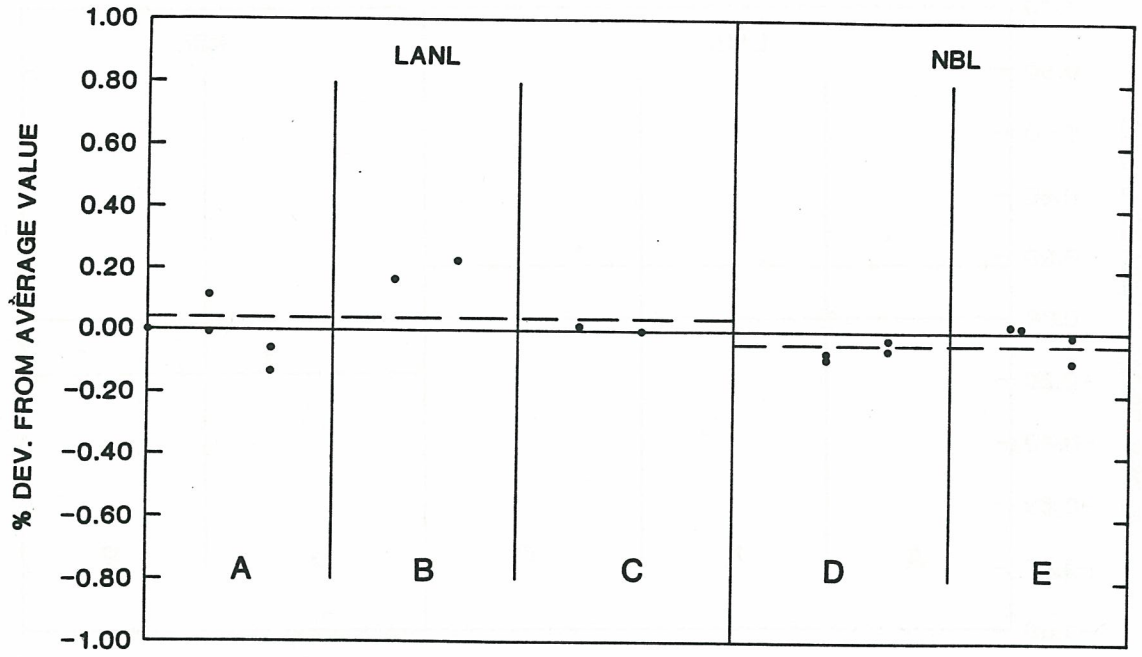

Fig. 5. Plot showing the scatter of the mass spectrometric values for the ^{235}U atom fractions in the samples from lot UISO-38 (~37.9 at.% ^{235}U).

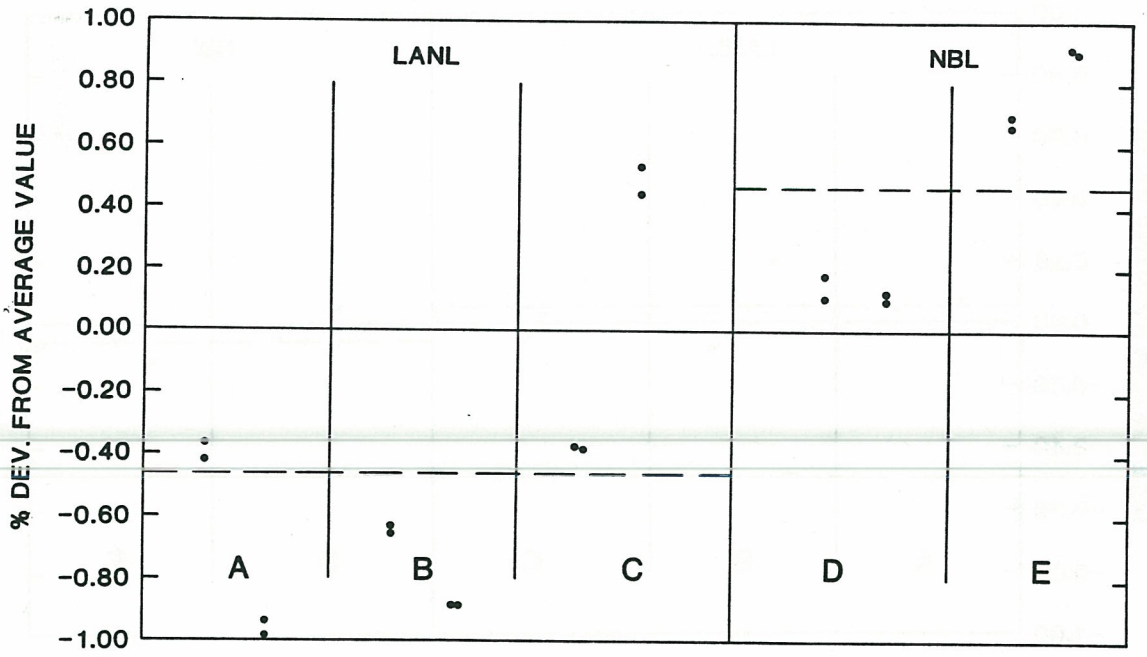

Fig. 6. Plot showing the scatter of the mass spectrometric values for the ^{235}U atom fractions in the samples from lot UISO-27 (~26.9 at.% ^{235}U).

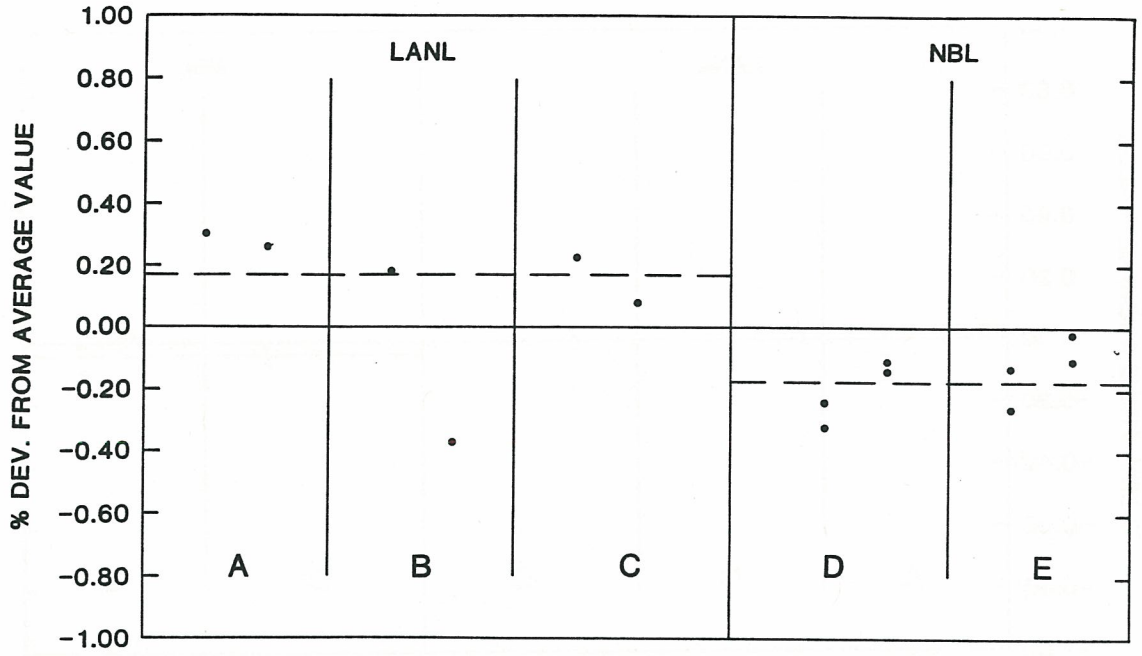

Fig. 7. Plot showing the scatter of the mass spectrometric values for the ^{235}U tom fractions in the samples from lot UISO-17 (~17.5 at.% ^{235}U).

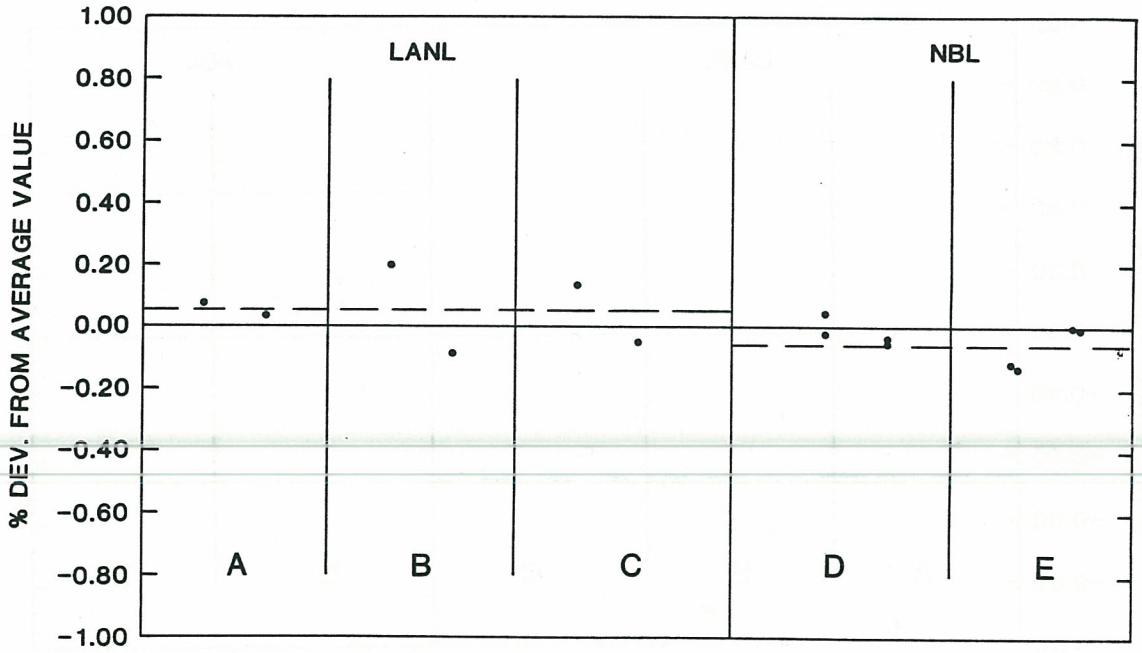

Fig. 8. Plot showing the scatter of the mass spectrometric values for the ^{235}U atom fractions in the samples from lot UISO-13 (~13.1 at.% ^{235}U).

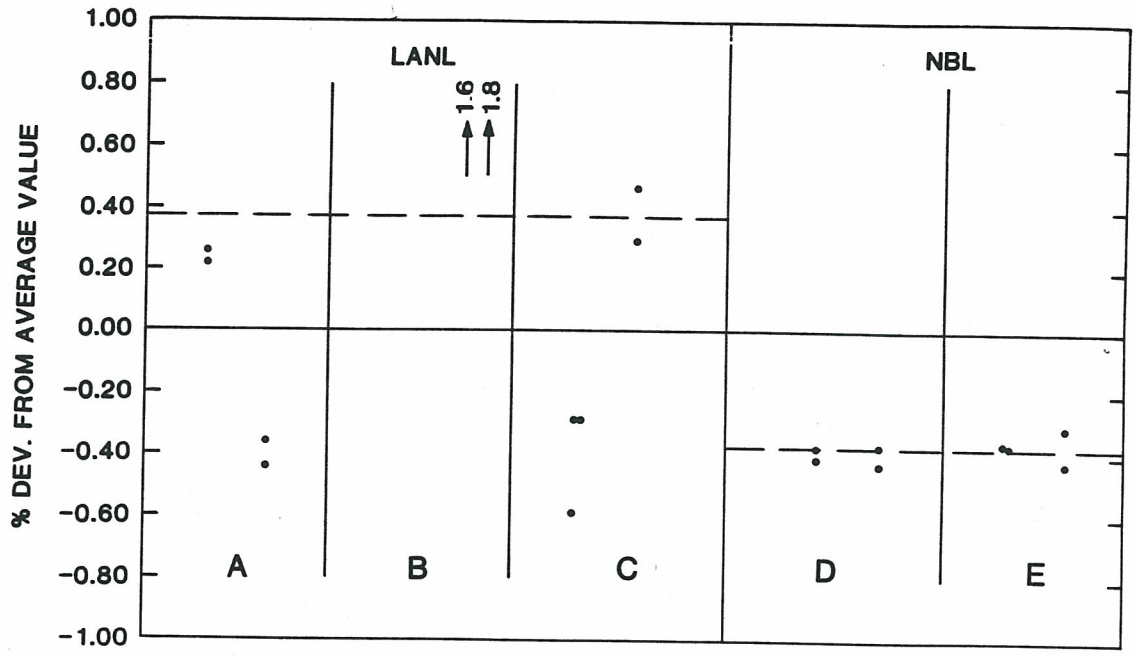

Fig. 9. Plot showing the scatter of the mass spectrometric values for the ^{235}U atom fractions in the samples from lot UISO-12 (~12.0 at.% ^{235}U).

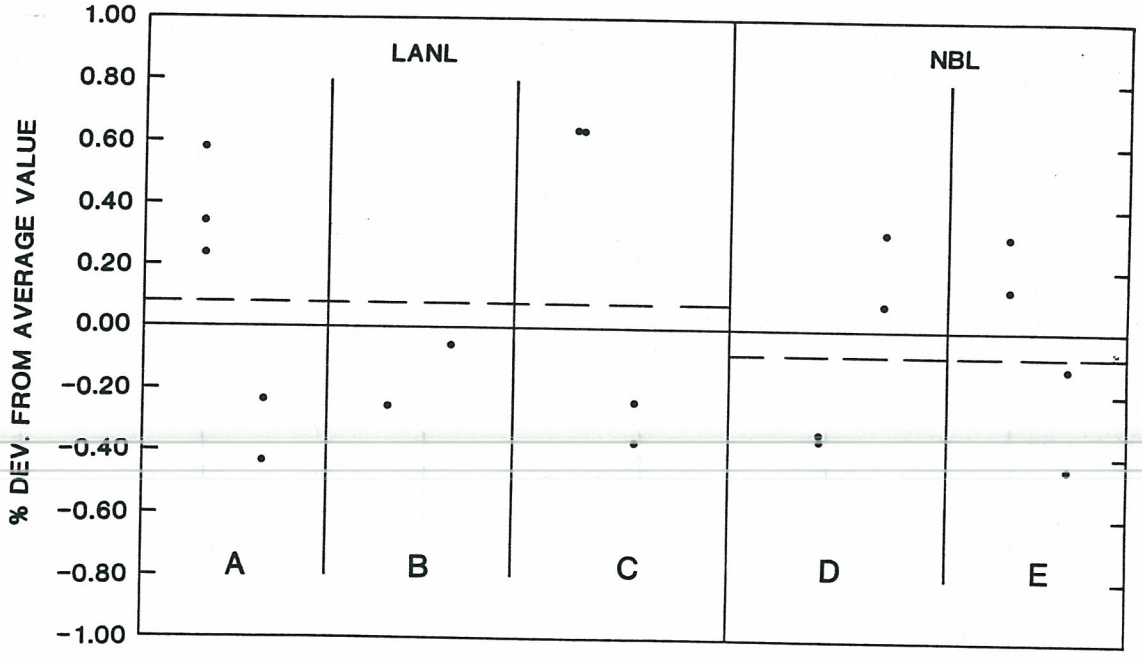

Fig. 10. Plot showing the scatter of the mass spectrometric values for the ^{235}U atom fractions in the samples from lot A1-323-1 (~10.3 at.% ^{235}U).

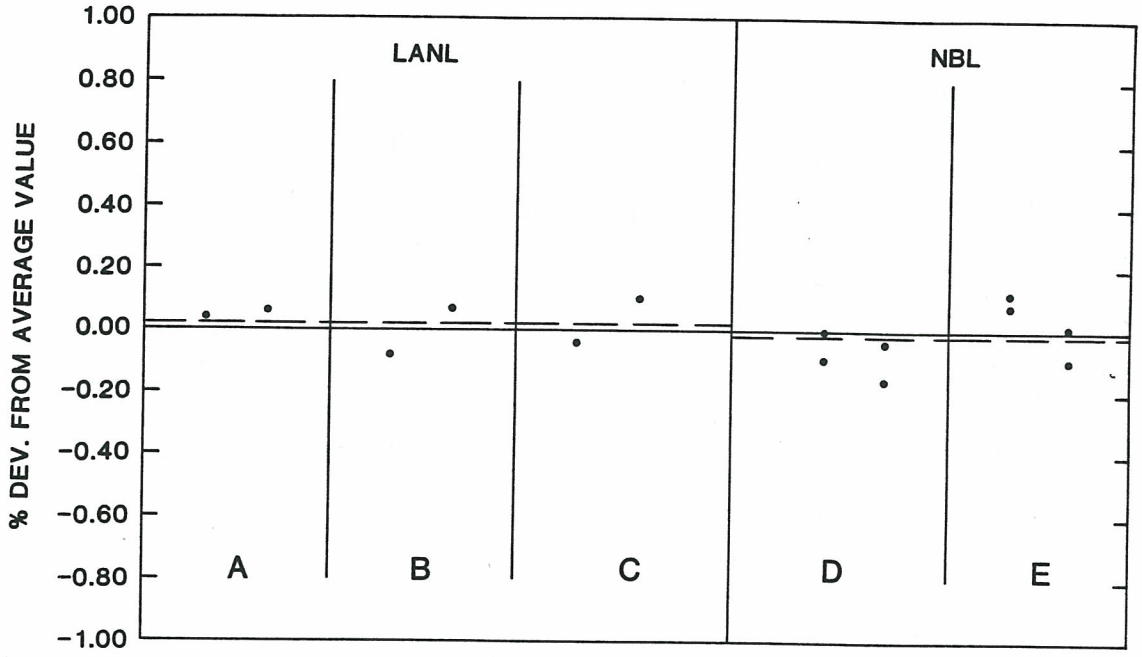

Fig. 11. Plot showing the scatter of the mass spectrometric values for the ^{235}U atom fractions in the samples from lot A1-324-1 (~10.2 at.% ^{235}U).

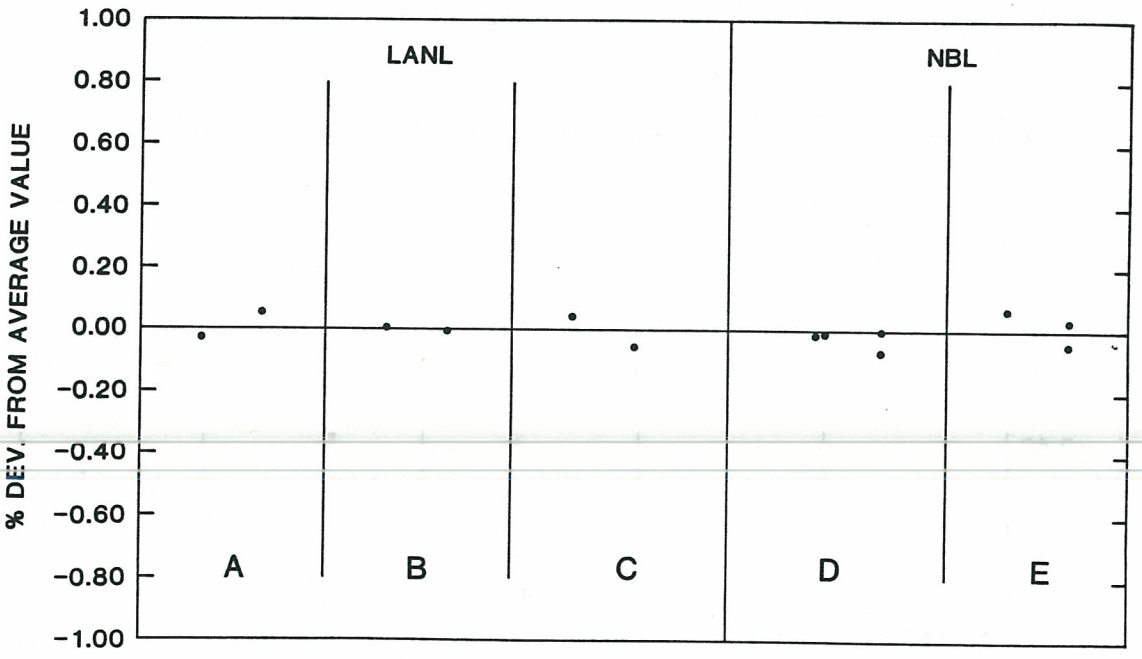

Fig. 12. Plot showing the scatter of the mass spectrometric values for the ^{235}U atom fractions in the samples from lot A1-324-2 (~10.2 at.% ^{235}U).

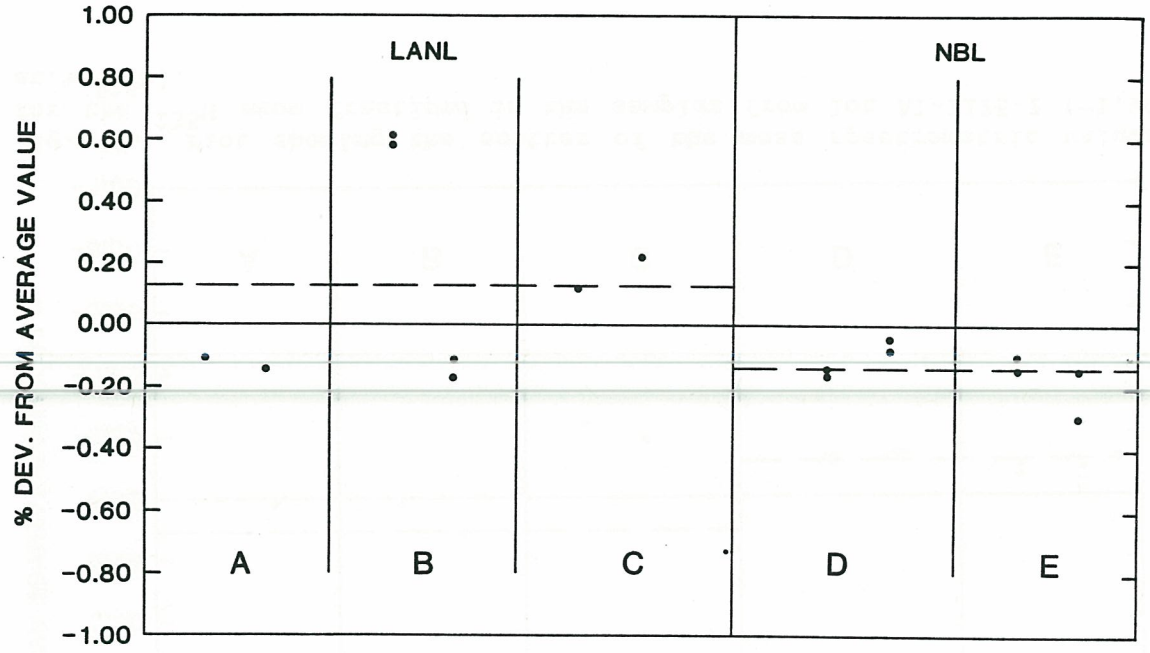

Fig. 13. Plot showing the scatter of the mass spectrometric values for the ^{235}U atom fractions in the samples from lot A1-1126-1 (~3.07 at.% ^{235}U).

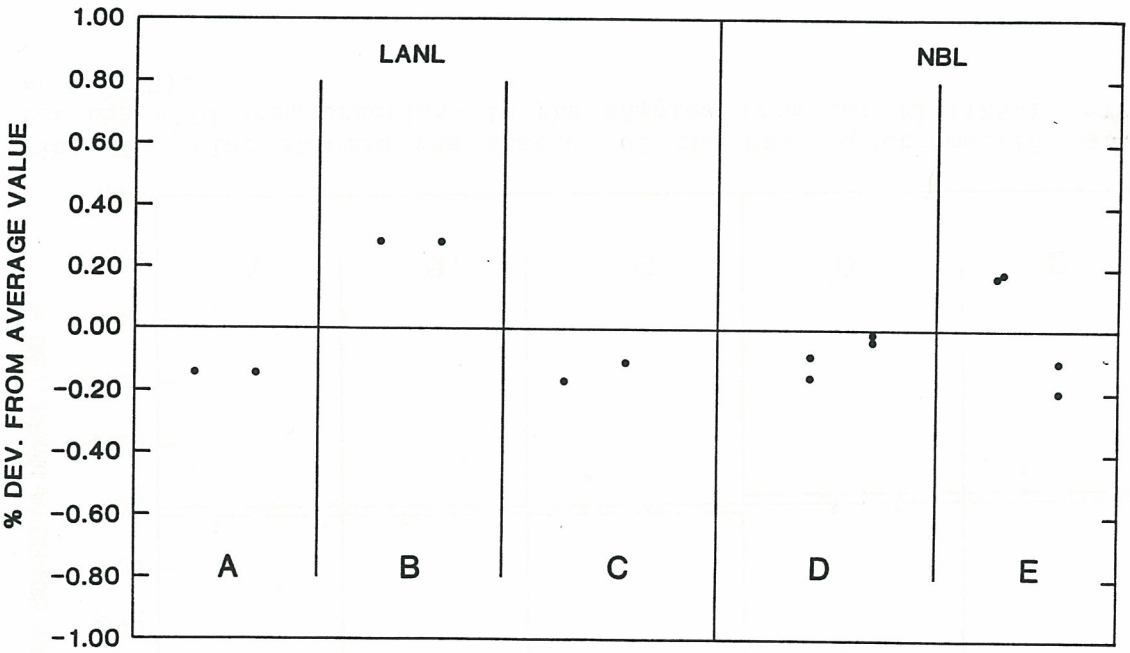

Fig. 14. Plot showing the scatter of the mass spectrometric values for the ^{235}U atom fractions in the samples from lot A1-1126-2 (~3.07 at.% ^{235}U).

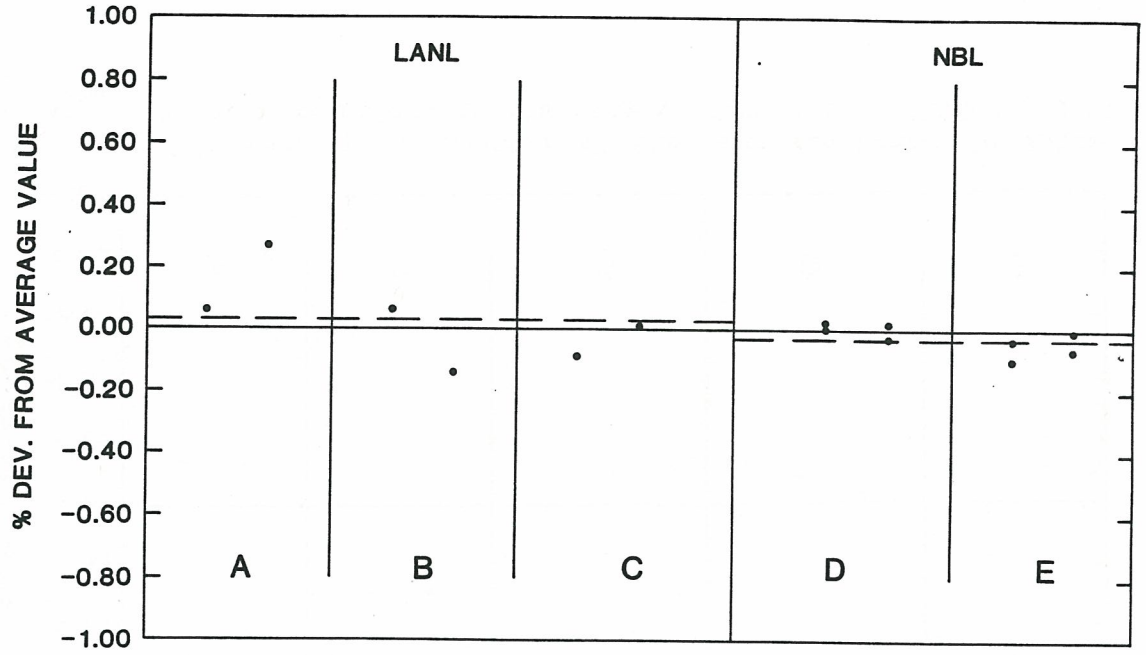

Fig. 15. Plot showing the scatter of the mass spectrometric values for the ^{235}U atom fractions in the samples from lot A1-1125-1 (~1.96 at.% ^{235}U).

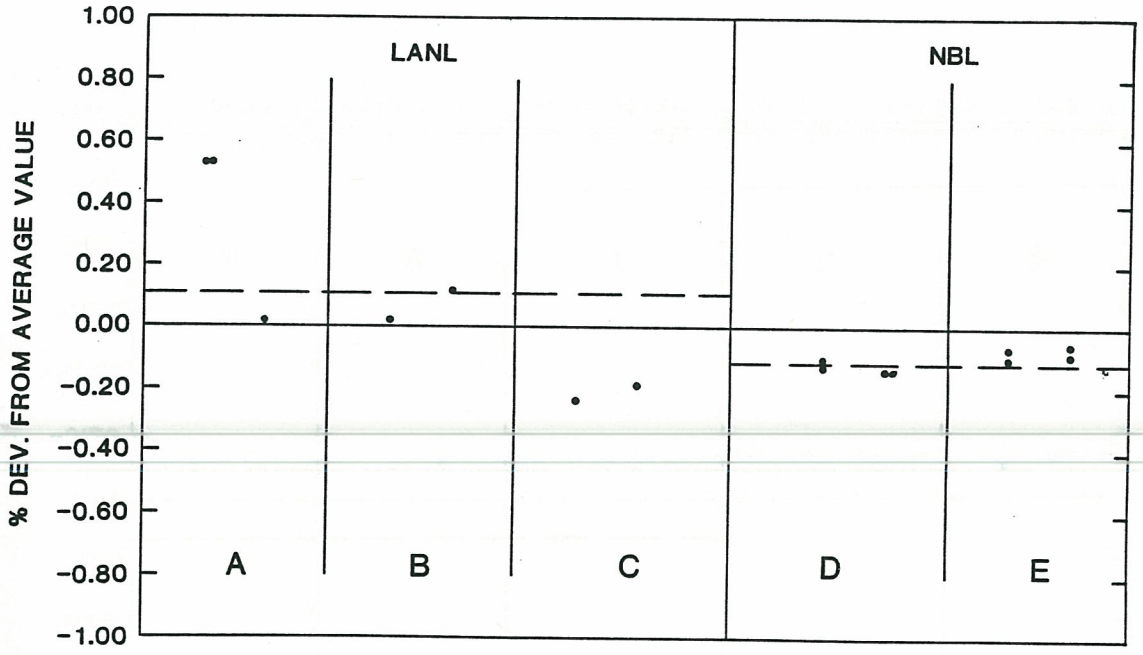

Fig. 16. Plot showing the scatter of the mass spectrometric values for the ^{235}U atom fractions in the samples from lot A1-1125-2 (~1.96 at.% ^{235}U).

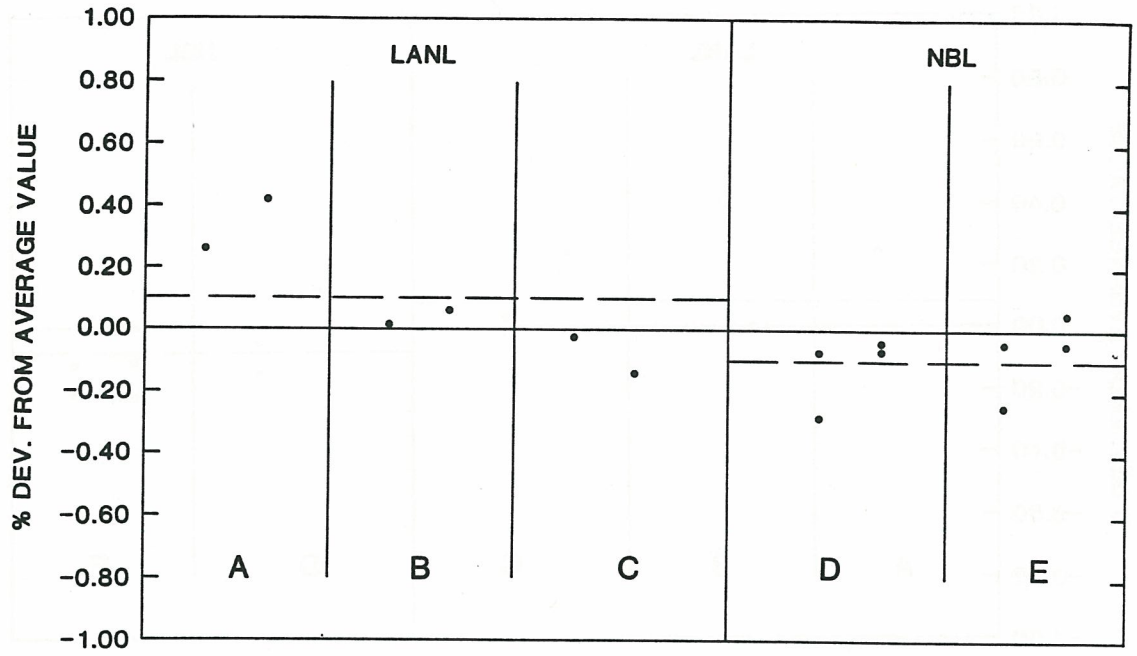

Fig. 17. Plot showing the scatter of the mass spectrometric values for the ^{235}U atom fractions in the samples from lot A1-1127-1 (~0.726 at.% ^{235}U).

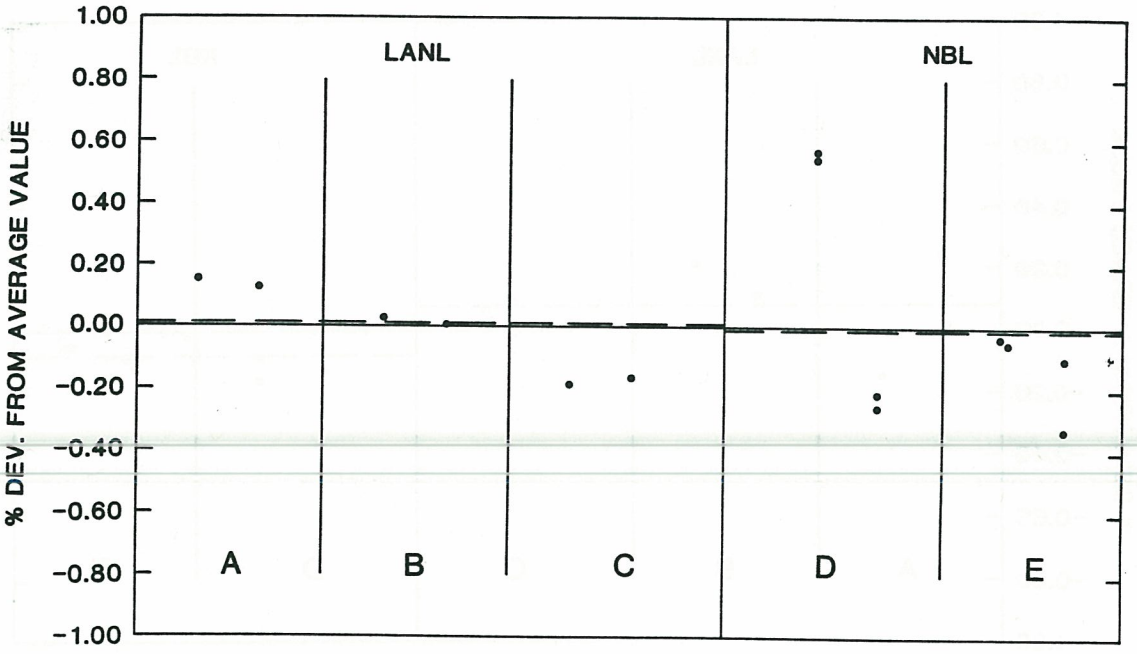

Fig. 18. Plot showing the scatter of the mass spectrometric values for the ^{235}U atom fractions in the samples from lot A1-1127-2 (~0.727 at.% ^{235}U).

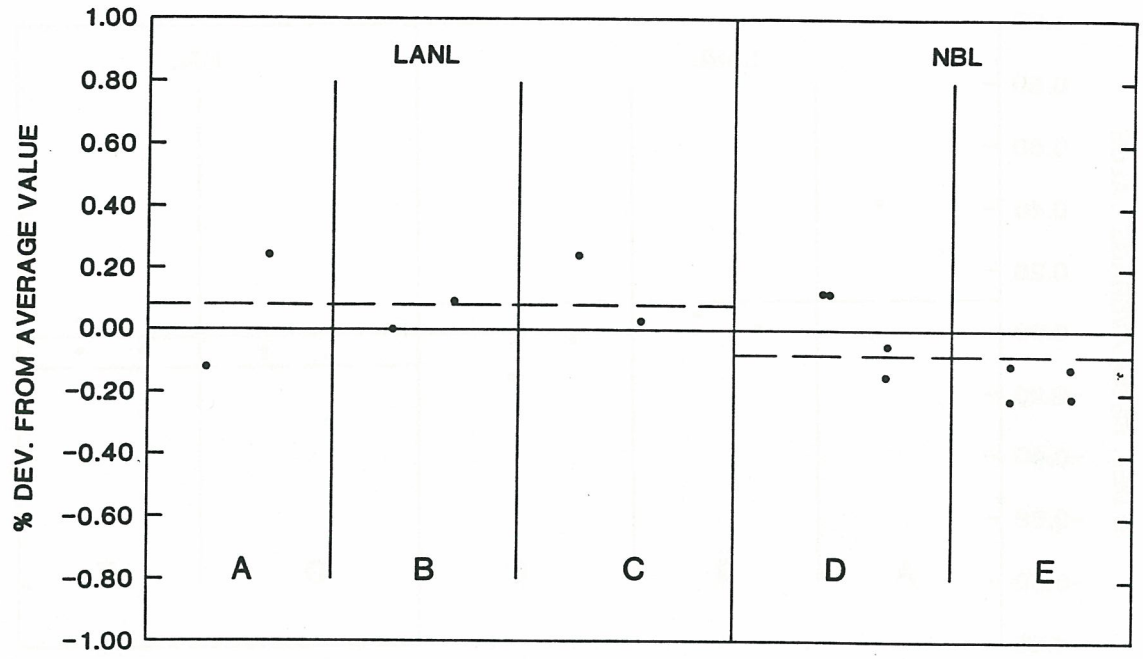

Fig. 19. Plot showing the scatter of the mass spectrometric values for the ^{235}U atom fractions in the samples from lot A1-408-2 (~0.722 at.% ^{235}U).

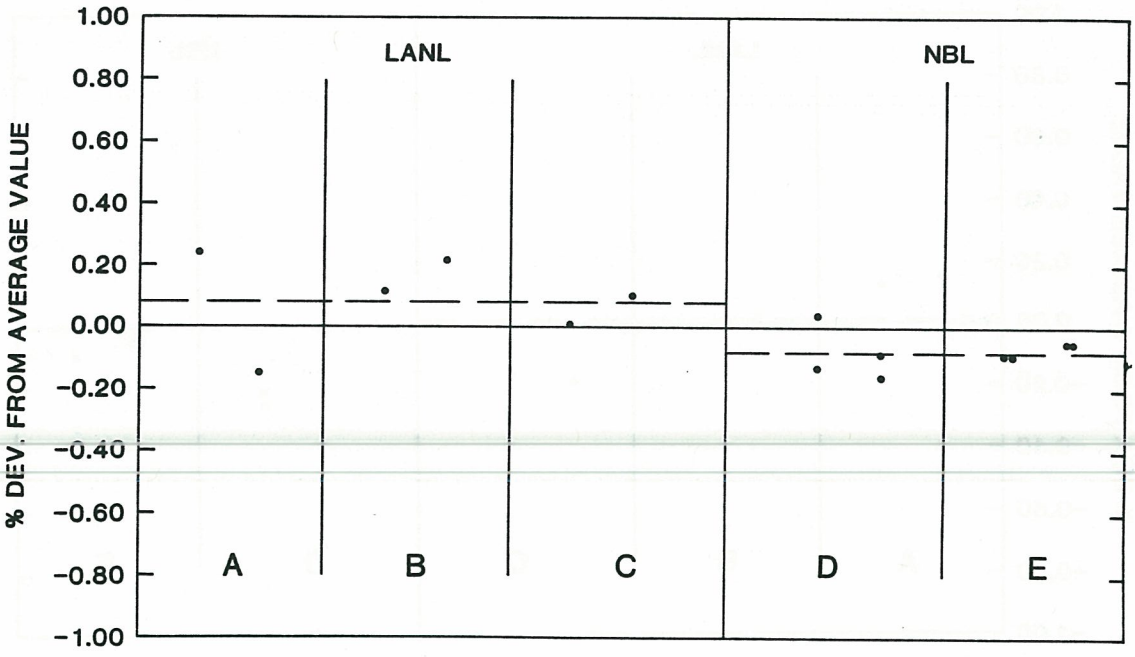

Fig. 20. Plot showing the scatter of the mass spectrometric values for the ^{235}U atom fractions in the samples from lot A1-409 (~0.721 at.% ^{235}U).

or immediately adjacent when the values are almost the same. The averages of LANL and NBL values are indicated by dashed lines across the LANL and NBL portions of the plots. It is clear in many cases that the scatter of values between subsamples is far greater than that between values from the same dissolved subsample. This condition is particularly dramatic for lots UISO-27 and UISO-12, for which both laboratories did two determinations on both dissolutions. The lots for which the results are most consistent are easily picked out by visual examination. It is observed that at the lower enrichments, the scatter of the values from the same dissolution is greater than at higher enrichments, as shown in Figs. 2 through 20. The increased scatter just demonstrates that the mass spectrometers involved had, for low enrichments, precisions (pure repeatability) for the ^{235}U fractions of a few hundredths of a percent, a more noticeable fraction of the absolute value than at the higher enrichments.

Figure 21 attempts to summarize much of the information in Table III and Figs. 2 through 20. In it, the percent deviations of LANL and NBL averages from their average are plotted with the %RSD values from Table III as error bars. The total distance between the LANL and NBL points is, of course, the magnitude of the value in the last column of Table III. An examination of the figure shows that for only seven lots of oxide are the two %RSD values and the differences between the LANL and NBL averages all <0.1%. Those seven lots, all with enrichments between 10 and 91%, are the obvious candidates to become a consistent set of enrichment standards, subject only to confirmation of consistency by gamma-ray spectroscopy. For several other containers of oxide, the difference between the LANL and NBL averages is <0.1%, but one or more of the associated %RSDs is >0.1%, indicating a degree of scatter in the measured values, which reduces confidence that the average atom fraction of ^{235}U has indeed been accurately determined by the analysis of the 10 subsamples dissolved.

Indeed, extracting from the many measured values of enrichment for each lot of oxide the "best" value, along with a valid estimate of the uncertainty in that "best" value, was clearly an important concern. Consequently, we submitted all the results to a LANL statistician who used the large statistical software package SAS to obtain the best weighted averages and estimates of error for all of the lots of oxide. Table IV presents the results of the SAS analysis, both the extracted enrichment value and its estimated error. Also included is the simple mean of the LANL and NBL average enrichment values. We

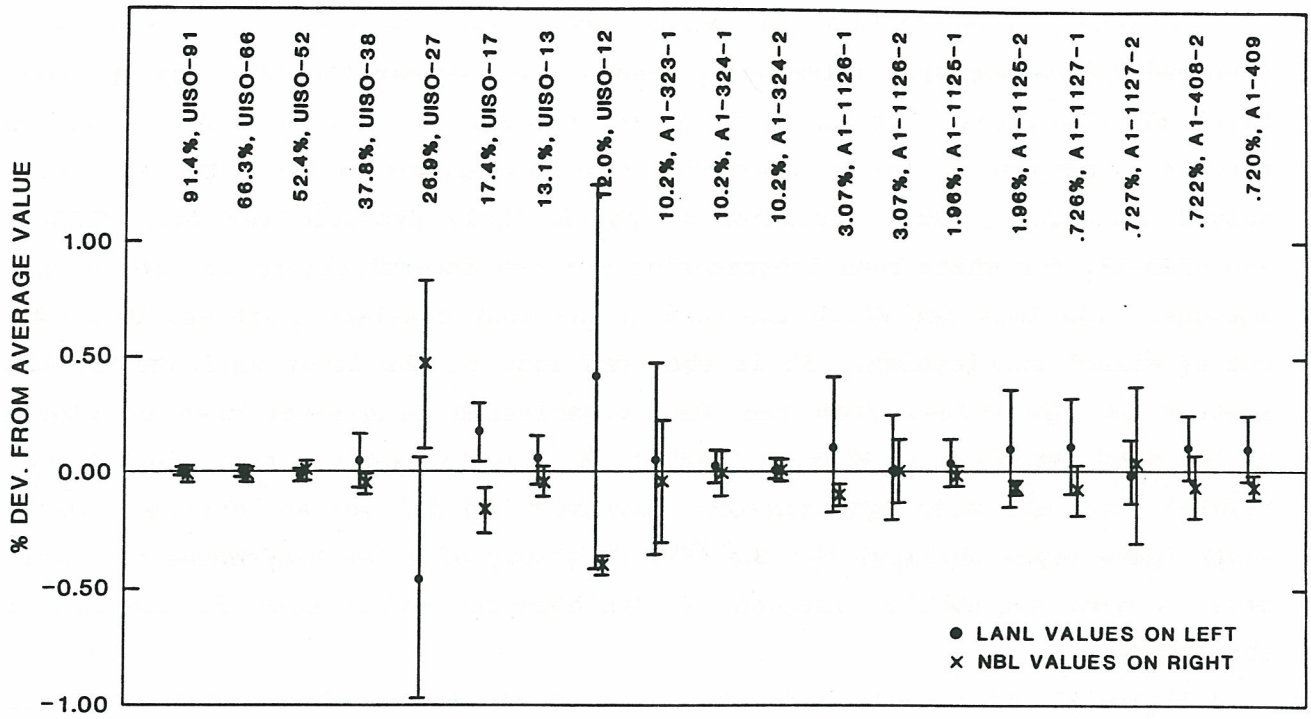

Fig. 21. For all 19 lots of uranium oxide, a plot of the percent deviations from their average of the LANL and NBL average ^{235}U atom fractions. The error bars are the computed RSD(%) of the measured values.

note that the first and second columns are nearly identical; thus, what the SAS package has done primarily is to produce an estimate of error. The third column of Table IV contains what are termed gamma-ray adjusted values for only some of the lots of oxide. Those lots given adjusted values are those that have estimated uncertainties of $\geq$0.1% or that are not consistent with gamma-ray measurements. This group will be regarded as secondary standards with the adjusted average enrichment values, while the group not given adjusted values will be used as primary standards with the SAS-generated average values, as described in Sec. I.D.

2. **Results of Analyses for Uranium Fractions**. Table V contains a summary of the NBL and LANL analyses for the uranium fraction (g U/g sample) of all the lots of oxide. The NBL values are the averages of independent analyses of six subsamples by the NBL Titrimetric Method, NBL-SA-U(E)-1, a modified Davies and Gray procedure. The values of %RSD are computed from the six measured values and, thus, have a large relative scatter among themselves even

TABLE IV

THREE DIFFERENTLY DERIVED VALUES OF AVERAGE ENRICHMENT
(at.%)

Standard ID	SAS Code Values and Uncertainty	Average NBL and LANL	Gamma-ray Adjusted Value
UISO-91	91.419 ± 0.011	91.419	
UISO-66	66.317 ± 0.032	66.317	
UISO-52	52.426 ± 0.004	52.425	
UISO-38	37.848 ± 0.015	37.852	
UISO-27	26.89 ± 0.13	26.91	27.00
UISO-17	17.455 ± 0.029	17.460	17.42
UISO-13	13.098 ± 0.008	13.098	
UISO-12	11.966 ± 0.044	11.959	11.93
A1-323-1	10.249 ± 0.017	10.245	10.22
A1-324-1	10.202 ± 0.003	10.203	
A1-324-2	10.200 ± 0.002	10.200	
A1-1126-1	3.070 ± 0.004	3.070	3.063
A1-1126-2	3.065 ± 0.003	3.065	3.065
A1-1125-1	1.962 ± 0.001	1.962	1.961
A1-1125-2	1.963 ± 0.002	1.962	1.962
A1-1127-1	0.7259 ± 0.0007	0.7260	0.7258
A1-1127-2	0.7271 ± 0.0007	0.7271	0.7256
A1-408-2	0.7218 ± 0.0006	0.7219	0.7226
A1-409	0.7204 ± 0.0006	0.7205	0.7190

though the absolute values are small. The average of the NBL %RSD values is in fact 0.04%, about what is expected of the method. Because of cost considerations, LANL used a less accurate gravimetric method for the uranium fraction, which had an estimated accuracy of 0.3%. This accuracy is nearly a factor of 10 worse than the NBL titrimetric method, so the NBL values will be accepted in the oxide characterizations. It should be noted here, though, as explained in detail later in this report (Sec. II.A.1), that for purposes of making the required chemical composition correction to gamma-ray spectrometric enrichment

TABLE V

NBL AND LANL URANIUM FRACTION VALUES

Standard ID	Nominal Enrichment (at.%)	NBL Mass Fraction g U/g Sample (wt%)	NBL %RSD (%)	LANL Mass Fraction g U/g Sample (wt%)	LANL %RSD[a] (wt%)	(NBL-LANL) • 100 / Average (%)
UISO-91	91	84.02	0.071	84.2	0.3	-0.21
UISO-66	66	84.52	0.032	84.7	0.3	-0.22
UISO-52	52	84.49	0.024	84.7	0.3	-0.24
UISO-38	38	84.58	0.034	84.7	0.3	-0.14
UISO-27	27	84.42	0.033	84.6	0.3	-0.21
UISO-17	17	84.63	0.035	84.8	0.3	-0.20
UISO-13	13	84.61	0.048	84.7	0.3	-0.11
UISO-12	12	84.60	0.015	84.8	0.3	-0.23
A1-323-1	10	84.19	0.036	84.5	0.3	-0.37
A1-324-1	10	84.40	0.061	84.7	0.3	-0.33
A1-324-2	10	84.41	0.062	84.7	0.3	-0.03
A1-1126-1	3	86.48	0.040	86.7	0.3	-0.03
A1-1126-2	3	86.71	0.030	87.0	0.3	-0.03
A1-1125-1	2	87.53	0.026	87.7	0.3	-0.02
A1-1125-2	2	87.61	0.040	87.7	0.3	-0.01
A1-1127-1	0.7	87.41	0.050	87.7	0.3	-0.03
A1-1127-2	0.7	87.05	0.034	87.3	0.3	-0.03
A1-409	0.7	85.05	0.087	85.2	0.3	-0.02
A1-408-2	0.7	85.03	0.071	85.2	0.3	-0.02

[a]The estimated accuracy of the gravimetric method.

measurements an accuracy of 0.3% is adequate. LANL did a gravimetric analysis of each of the three samples from each lot, and in nearly every case all three values agreed in all of the three significant figures reported. We see from Table V that in every case the LANL final value is less than the NBL value, but it is comforting that in all but two cases the difference is less than the 0.3% accuracy claimed by the gravimetric method. In the two remaining cases the difference is just slightly >0.3%. The conclusion is that the two sets of measurements are consistent within the estimated accuracies of the methods.

3. Results of Emission Spectrometric Analyses. The results of the emission spectrographic analyses are given in Table VI. For all elements included

TABLE VI

RESULTS OF EMISSION SPECTROGRAPHIC ANALYSES OF ENRICHMENT STANDARDS[a,b]
(mg/g)

Standard ID	Ag	Al	B	Ba	Be	Bi	Ca	Cd	Cr	Cu	Li	Mg	Mn	Mo	Na	Ni	P	Pb	Sb	Si	Sn	Sr	V	Zn
UISO-91	<1	<5	<0.2	<5	<0.2	2	5	<2	5	5	<0.2	5	<1	<25	30	5	<100	2	<5	25	1	<20	<25	<25
UISO-66	<1	<5	<0.2	<5	<0.2	<2	5	<2	5	10	<0.2	2	<1	<25	15	5	<100	2	<5	20	2	<20	<25	<25
UISO-52	15	<5	<0.2	<5	<0.2	<2	5	<2	5	7	<0.2	1	<1	<25	30	5	<100	1	<5	150	2	<20	<25	<25
UISO-38	<1	20	0.3	<5	<0.2	<2	10	<2	5	10	<0.2	1	<1	<25	35	5	<100	4	<5	20	2	<20	<25	<25
UISO-27	<1	70	0.3	<5	<0.2	<2	20	<2	7	5	<0.2	5	<1	<25	50-500	5	<100	2	<5	30	2	<20	<25	<25
UISO-17	15	30	0.3	<5	<0.2	<2	5	<2	3	5	<0.2	5	<1	<25	30	5	<100	2	<5	25	8	<20	<25	<25
UISO-13	<1	<5	0.3	<5	<0.2	30	5	<2	<1	7	<0.2	2	<1	<25	30	5	100	100	<5	15	8	<20	<25	<25
UISO-12	<1	<5	0.3	<5	<0.2	<2	5	<2	3	100	<0.2	2	<1	<25	30	5	<100	2	<5	20	8	<20	<25	<25
A1-323-1	<1	20	0.7	<5	<0.2	<2	5	<2	<1	10	<0.2	80	2	<25	2	5	<100	2	<5	500	<2	<20	<25	<25
A1-324-1	10	10	0.7	<5	<0.2	<2	5	<2	<1	4	<0.2	15	2	<25	2	10	<100	2	<5	300	15	<20	<25	<25
A1-324-2	1	10	0.5	<5	<0.2	<2	5	<2	<1	4	<0.2	10	2	<25	2	5	<100	2	<5	300	10	<20	<25	<25
A1-1126-1	5	5	<0.2	<5	<0.2	<2	5	<2	30	1	<0.2	3	2	<25	10	60	100	2	<5	30	30	<20	<25	<25
A1-1126-2	<5	5	<0.2	<5	<0.2	<2	5	<2	30	1	<0.2	2	2	<25	8	40	100	20	<5	30	30	<20	<25	<25
A1-1125-1	4	<5	0.2	<5	<0.2	<2	5	<2	10	4	<0.2	2	1	<25	2	30	<100	2	<5	10	2	<20	<25	<25
A1-1125-2	<1	<5	<0.2	<5	<0.2	<2	5	<2	10	4	<0.2	1	1	<25	2	30	<100	<1	<5	8	15	<20	<25	<25
A1-1127-1	<1	10	<0.2	<5	<0.2	<2	5	<2	10	1	<0.2	2	<1	<25	7	10	100	20	<5	15	10	<20	<25	<25
A1-1127-2	<1	30	0.3	<5	<0.2	<2	5	<2	10	1	<0.2	100	<1	<25	10	20	200	<2	<5	100	15	<20	<25	<25
A1-409	<1	400	1	<5	<0.2	<2	5	<2	10	2	<0.2	20	5	<25	30	5	<100	<1	<5	30	2	<20	<25	<25
A1-408-2	1	200	1	<5	<0.2	<2	5	<2	10	2	<0.2	20	10	<25	30	10	<100	2	<5	30	5	<20	<25	<25

[a]All results expressed as <n mean that the concentration of the element in question is below the sensitivity of the spectrographic system, which is n mg/g for that element.
[b]Results expressed without the < symbol generally have a factor of 2 accuracy and precisions of %50% RSD.

in the analyses, the results are given in micrograms of the element per gram of sample. The meaning of results preceded by the symbol < is that the particular element was not detected and that the sensitivity of the measurement is as given in the entry. All other results are thought to be accurate within a factor of 2 and to have precisions of ~50% RSD. As mentioned above, the reason for doing these analyses was to be assured that the level of minor elemental impurities was low enough to be ignored in the chemical composition correction term to be explained in detail in Sec. II.A.1. As a rule of thumb, if the sum of the concentrations of elements with Z < 30 is <1% of total mass and if the sums of the concentrations of elements with Z > 30 is <0.1% of total mass, the effect on the gamma-ray measurements of the enrichments will be <0.1%. For all 19 lots of oxide, the sums of the concentrations fall far below these guidelines, even if undetected elements are assumed to be present at their sensitivity levels. We are sure that impurities in the lots of uranium oxide will not cause any measurement errors greater than a few hundredths of a percent at most.

D. Comparison with Gamma-Ray Measurements and Designation of Primary and Secondary Standards

The relatively large variation of the enrichment among samples of ~30-mg from some of the lots of oxide and the correspondingly rather large uncertainties of the average values derived by SAS for those lots leaves a real probability that the "final" average of the mass spectroscopic values is indeed significantly biased. Inasmuch as gamma-ray measurements sample ~30 g of oxide, about a thousand times more than a single mass spectrometer measurement, it is probable that the gamma-ray method can provide better relative measurements of the average enrichment for some of the lots than have been obtained by the dissolution of ten 30-mg samples. As explained in Sec. II.A.3, if the appropriately corrected (for chemical composition and attenuation in the packages) total measured rate of the 185.7-keV gamma ray from ^{235}U is divided by the enrichment, one should obtain a constant value for all the 19 containers of oxide. Figure 22 presents a comparison of such measurements. In each case, the appropriate rate has been divided by the SAS-generated average enrichment, and the percent deviation of those values from the value of the 17%-enriched lot has been plotted on the vertical axis. The 17% package was chosen because it has been used as a consistency check source throughout all the work, and

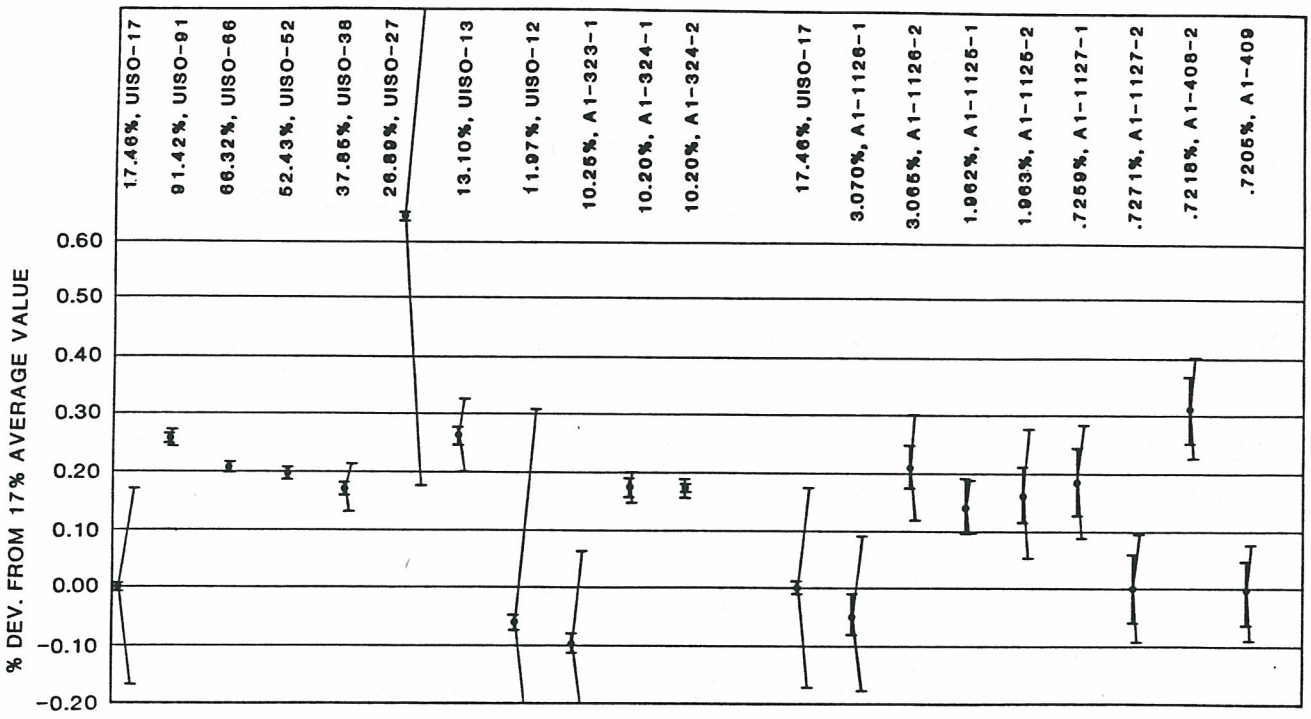

Fig. 22. For all 19 lots of uranium oxide, a comparison of the ratios of the total corrected count rate and the best mass spectrometric determination of the ^{235}U atom fraction. The comparisons are given as percent deviations from the average value from the 17%-enriched lot. The straight error bars indicate the gamma-ray counting precision and the angled error bars indicate the scatter of the mass spectrometer values. If both gamma-ray counting and mass spectrometrically determined values were perfect all points would lie on the 0.0 line.

the constant from counting it had a very small statistical variation. The vertical error bars in Fig. 22 are the estimates of uncertainty from the gamma-ray counting and in all cases are under 0.1% for the higher-enriched lots, and usually under 0.05%. The angled uncertainty bars are the SAS-estimated errors. An examination of Fig. 22 shows that the seven lots of oxide with the smallest error bars for both gamma-ray counting and mass spectrometric determinations are consistent within a range of ±0.05%. Fortunately, those 7 lots span the range from 91% down to 10% enrichment, and it is gratifying that those lots, which had the smallest variation of measured enrichment among the small ~30-mg samples, show the highest degree of consistency with the gamma-ray measurements. For these 7 lots of oxide, there is no reason to doubt that the SAS-generated average value of the mass spectrometric results is the best value of the average enrichment that can be obtained, and they will be designated as the primary working enrichment standards within the set of 19 recharacterized

lots of oxide. Table VII gives the enrichments and all other pertinent parameters pertaining to the primary standards. The remaining 12 lots will be designated as secondary standards, and the enrichments (^{235}U atom fraction) have been adjusted to make the gamma-ray counting measurements on them consistent with the 7 primary standards. The adjustments range from ~0.4% to essentially nothing. As seen from Fig. 22, the plotted points for a few of the secondary standards fall within the range of the primary standards. They are designated as secondary standards because of their greater error bars for both gamma-ray counting statistics and mass spectrometer determinations. Table VIII contains all pertinent parameters pertaining to the secondary standards. It should be emphasized that the atom fractions of ^{234}U, ^{236}U, and ^{238}U are only nominal in both Tables VII and VIII and are provided for users who may use the standards for measurements other than enrichment. No attempt has been made to analyze all the mass spectrometric data for those isotopes, nor to make the sum of all the isotopes as given in the the two tables add to 100%.

II. DEMONSTRATION OF ENRICHMENT MEASUREMENT CAPABILITY

A. Experimental Procedures

1. Review of the Measurement Physics and the Required Corrections. The determination of the ^{235}U atom fraction in uranium--usually termed the enrichment--by gamma-ray spectrometry has become a much-used and well-developed NDA technique. The principles involved were completely outlined as early as 1970.[1] Other reports, papers, and private communications in the years since have described the development of procedures, the more accurate elucidation of the principles, and the quantification of possible interferences. References 2, 3, and 4 are a few of them. In 1985, Matussek published the most complete and accurate description of both principles and procedures thus far given,[5] which was written as a user's manual for the Certified Reference

TABLE VII

IMPORTANT PARAMETERS OF PRIMARY ENRICHMENT STANDARDS

Standard ID	Accepted Value ^{235}U (at.%)	Std Dev	Nominal Values ^{234}U (at.%)	^{236}U (at.%)	^{238}U (at.%)	Oxide Mass (g)	Mass Fraction g U/g Sample (wt%)	Mass U (g)	Mass Fraction $^{235}U/U$ (wt%)	Mass ^{235}U (g)	Bottom Thickness (cm)	Lid Thickness (cm)	Approx. Oxide Depth (cm)	Approx. Oxide Density (g/cm^3)
UISO-91	91.419 ±	0.011	0.915	0.334	7.33	1178	84.02	990	91.336	904	0.0217	0.0269	7.7	1.7
UISO-66	66.317 ±	0.032	0.583	0.259	32.8	1171	84.52	990	66.040	658.8	0.0215	0.0271	5.6	2.3
UISO-52	52.426 ±	0.004	0.536	0.869	46.2	1171	84.49	989	52.117	515.4	0.0217	0.0282	5.8	2.2
UISO-38	37.848 ±	0.015	0.263	0.218	61.6	1172	84.58	991	37.552	372.1	0.0212	0.0277	6.0	2.1
UISO-13	13.098 ±	0.008	0.084	0.102	86.7	1171	84.61	991	12.955	128.4	0.0213	0.0282	5.4	2.4
A1-324-1	10.202 ±	0.003	0.052	0.091	89.7	1170	84.40	987	10.087	99.6	0.0243	0.0282	4.6	2.8
A1-324-2	10.200 ±	0.001	0.053	0.091	89.7	1169	84.41	987	10.085	99.5	0.0211	0.027	4.1	3.1

TABLE VIII

IMPORTANT PARAMETERS OF SECONDARY ENRICHMENT STANDARDS

Standard ID	Adjusted Value ^{235}U	Nominal Values ^{234}U (at.%)	^{236}U (at.%)	^{238}U (at.%)	Oxide Mass (g)	Mass Fraction g U/g Sample (wt%)	Mass U (g)	Mass Fraction $^{235}U/U$ (wt%)	Mass ^{235}U (g)	Bottom Thickness (cm)	Lid Thickness (cm)	Approx. Oxide Depth (cm)	Approx. Oxide Density (g/cm^3)
UISO-27	27.0	0.237	0.271	72.7	1174	84.42	991	26.75	265.0	0.0213	0.0279	6.2	2.1
UISO-17	17.42	0.140	0.169	82.2	1169	84.63	989	17.24	171.0	0.0212	0.0275	5.0	2.6
UISO-12	11.93	0.073	0.116	87.8	1170	84.60	990	11.80	117.0	0.0208	0.0275	5.4	2.4
A1-323-1	10.22	0.054	0.092	89.6	1120	84.19	943	10.10	95.3	0.0213	0.0270	3.9	3.1
A1-1126-1	3.063	0.025	0.016	96.9	1003	86.48	867	3.025	26.20	0.0214	0.0275	4.4	2.5
A1-1126-2	3.065	0.025	0.017	96.9	984	86.71	853	3.028	25.80	0.0206	0.0268	4.3	2.5
A1-1125-1	1.961	0.016	0.009	98.0	959	87.53	839	1.936	16.20	0.0221	0.0275	3.5	3.0
A1-1125-2	1.962	0.016	0.009	98.0	976	87.61	855	1.938	16.60	0.0209	0.0275	3.5	3.1
A1-1127-1	0.7258	0.005	0.002	99.3	1022	87.41	893	0.7167	6.40	0.0213	0.0281	4.5	2.5
A1-1127-2	0.7256	0.005	0.002	99.3	1041	87.05	906	0.7165	6.49	0.0219	0.0280	4.4	2.6
A1-408-2	0.7226	0.005	<0.001	99.3	1339	85.03	1139	0.7135	8.13	0.0215	0.0280	5.7	2.6
A1-409	0.7190	0.005	<0.001	99.3	1361	85.05	1158	0.7100	8.22	0.0210	0.0280	5.7	2.6

Materials EC-NRM-171/NBS-SRM-969, the recently released set of low-enrichment standards for gamma-ray determinations of enrichment.* In spite of the abundance of published reference material, it seems useful to give here a simplified derivation and fairly complete discussion of the fundamental equations so that the nature of the several required corrections can be clearly seen and the procedures adopted herein to test the self-consistency and accuracy of the LANL working standards can be justified.

Before doing so, we briefly discuss mass and linear attenuation coefficients, both for single elements and for combinations of elements. The mass attenuation coefficient for an element may be written as

$$\mu^m = N \sigma / A_e \quad , \tag{1}$$

where N = Avogadro's number,

A_e = the average atomic mass for the isotopic distribution of the particular elemental sample, and

σ = the total atomic cross section for photon interaction, being a function of both Z and photon energy.

The point to be emphasized here is that A_e is not necessarily a constant, but may change if the isotopic distribution changes from sample to sample. For uranium this is very much the case. For natural uranium $A_e \approx 238$, while for

---

*The reference material EC-NRM-171/NBS-SRM-969 is the result of a major international cooperative project. The following organizations took part in its development:

the European Safeguards Research and Development Association NDA Working Group,
the Commission of the European Communities,
-Joint Research Centre,
Central Bureau for Nuclear Measurements, Geel, and
-Joint Research Centre, Ispra
the U.S. National Bureau of Standards, and
the U.S. Department of Energy
-NBL.

The set consists of five standards with ^{235}U fractions between 0.3% and 4.5%, all certified with accuracies of $\leq$0.1% relative.

very highly enriched uranium $A_e \approx 235$, a difference of ~1.3%, which should be considered when striving for the most accurate enrichment measurements. Now by definition the linear attenuation coefficient for an element is given by

$$\mu^{\ell} = \mu^{m} \rho \quad , \tag{2}$$

where ρ is the actual spatial density of the elemental sample. The mass attenuation coefficients are usually tabulated because they are constants (almost) for the elements not depending on density. It is easily shown that, for a mixture of elements, the linear attenuation coefficient is given by

$$\mu^{\ell} = \Sigma \, \mu_i^{m} \rho_i \quad , \tag{3}$$

where μ_i^{m} and ρ_i are the mass coefficients and actual spatial densities for the individual constituents. Similarly, the mass attenuation coefficient for a mixture of elements is given by

$$\mu^{m} = \Sigma \, \mu_i^{m} f_i \quad , \tag{4}$$

where f_i is the mass fractions of elements in the mixture and as before μ_i^{m} is the mass attenuation coefficients of the individual elements.

A fundamental quantity involving the attenuation coefficients is the fraction of gamma rays passing through a layer of material unabsorbed and unscattered. In this report, that fraction is called the transmission and is given by

$$T = e^{-\mu^{m} \rho t} = e^{-\mu^{\ell} t} \tag{5}$$

for a layer of thickness t, density ρ and mass attenuation coefficient μ^m, remembering that $\mu^\ell = \mu^m \rho$. A useful compilation of attenuation coefficients is that of Hubbell,[6] which also contains much explanatory material by way of definition, measurement evaluation, theoretical computation, and accuracies for the tabulated values.

Figure 23 is a schematic of a rather impractical far-field geometrical arrangement for enrichment measurement, but one for which the simple one-dimensional expressions would be an excellent approximation. As seen, a detector (assumed to be a high-resolution one) views a package of uranium compound through a collimator so that it sees a fixed area of the sample. With the conditions given on the relative dimensions, all the detected gamma rays travel in nearly parallel paths normal to the package wall along the common axis of the collimator and detector. Inasmuch as the 185.7-keV gamma ray from the alpha decay of ^{235}U is by far the most intense of those emitted* and is almost

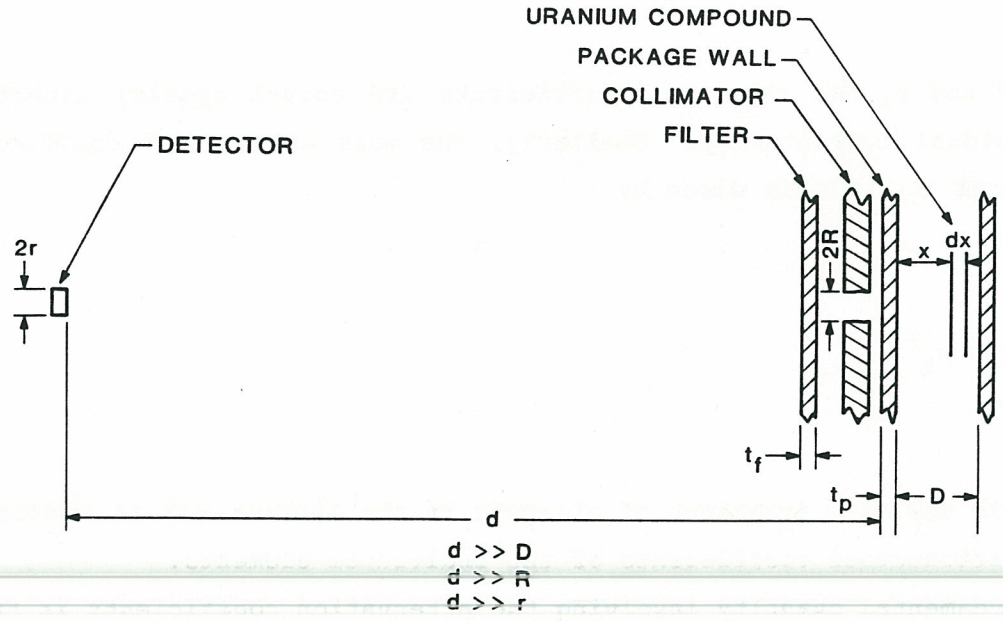

Fig. 23. A schematic of an idealized (but quite impractical) geometry for gamma-ray measurements of uranium enrichment upon which a useful one-dimensional derivation of the pertinent equations may be based.

*The 185.7-keV gamma ray is emitted in 57.5 ± 0.9% of ^{235}U decays. With a ^{235}U half-life of (7.038 ± 0.007) • 10^8 years, the emission rate per unit mass is computed as (4.60 ± 0.07) • 10^4/s-g ^{235}U.

universally used for enrichment measurements, it will be assumed in all that follows that the 185.7-keV gamma ray is being used. With these constraints and assumptions, we can write a one-dimensional integral expression for the full-energy interaction rate of the 185.7-keV gamma ray in the detector as

$$FEIR = (\Omega_d/4\pi)\varepsilon_I \Lambda(N/A_u)\, \rho_u E\, I\, A\, (e^{-\mu_f^m \rho_f t_f})(e^{-\mu_p^m \rho_p t_p}) \int_o^D e^{-\mu^\ell x} dx \quad , \qquad (6)$$

where FEIR = full-energy interaction rate,

Ω_d = the solid angle subtended by the detector from the collimator,

ε_I = the intrinsic full-energy efficiency of the detector at 185.7 keV,

Λ = the decay constant for ^{235}U,

N = Avogadro's number,

A_u = the average atomic mass of the uranium in the sample,

ρ_u = the actual spatial density of uranium in the compound,

E = the enrichment, the fraction of uranium atoms that is the isotope ^{235}U,

I = the fraction of ^{235}U decays giving rise to the 185.7-keV gamma ray,

A = the area of the collimator,

μ_f^m, ρ_f = the mass attenuation coefficient and density of the filter,

μ_p^m, ρ_p = the mass attenuation coefficient and density of the package, and

μ^ℓ = the linear attenuation coefficient of the uranium compound.

It should be noted that the product $\Omega_d\varepsilon_I/4\pi$ is the fraction of gamma rays from a point source at the collimator that produce full-energy interactions in the detector; that the product $\Lambda NEI/A_u$ is the rate of 185.7-keV decays per gram of compound; that $e^{-\mu_f^m \rho_f t_f}$ is the transmission through the filter (T_f); and that $e^{-\mu_p^m \rho_p t_p}$ is similarly the transmission through the sample package (T_p). On evaluation, the integral

$$\int_o^D e^{-\mu^{\ell} x} dx = (1/\mu^{\ell})(1 - e^{-\mu^{\ell} D}) = (1/\mu^{\ell})(1 - T_s) \quad , \tag{7}$$

where T_s is the transmission through the uranium compound. Now the linear attenuation coefficient of the uranium compound

$$\mu^{\ell} = \mu_u^{\ m} \rho_u + \mu_M^{\ m} \rho_M \ , \tag{8}$$

where $\mu_u^{\ m}$ = the mass attenuation coefficient of uranium at 185.7 keV,

ρ_u = the actual spatial density of uranium in the compound,

$\mu_M^{\ m}$ = the mass attenuation coefficient of the matrix, which is everything else in the compound, also at 185.7 keV,

ρ_M = the actual spatial density of the matrix materials.

Substituting the above results and rearranging the expression in Eq. (6) we get

$$FEIR = [(\Omega_d/4\pi)\varepsilon_I \Lambda (1/\sigma) I \ A \ T_f] \ E \ T_p (1 - T_s)/[1 + (\mu_M^{\ m}/\mu_u^{\ m})(\rho_M/\rho_u)] \quad . \tag{9}$$

Now all the parameters within the leftmost square bracket in Eq. (9) are constants for a given measurement geometry, and if their values were known, enrichment measurements could be done without the use of physical standards. In practice, of course, the known or computed values of some of the parameters are so uncertain that enrichment values cannot be determined with the usually desired accuracies by that method. Instead, the value of the product of all the parameters is determined by the use of physical standards, becoming essentially

the calibration constant for the particular counting geometry. Letting that constant be K, the final equation becomes

$$FEIR = \frac{K\ E\ T_p(1 - T_s)}{[1 + (\mu_M^m/\mu_u^m)(\rho_M/\rho_u)]} \quad . \tag{10}$$

The three terms $(1 - T_s)$, T_p, and $[1 + (\mu_M^m/\mu_u^m)(\rho_M/\rho_u)]$ are essentially correction terms, which are computed from the known properties of the uranium compound and its package. Most often enrichment measurements are made on samples for which T_s is zero, though that is not required if T_s can be measured or calculated. The condition $T_s = 0$ is usually described by saying that the sample is infinitely thick, which means that addition of more material will not increase the observed count rate. For all the LANL standards described in this report $T_s = 0$, so the term will be eliminated from all expressions given below. The term, T_p, must be accurately known if accurate values of enrichment are to be determined. Though in narrow field geometries such as shown in Fig. 23, T_p may be computed with sufficient accuracy from known values of the composition, thickness, and density of the package, that will not generally be possible. In near-field geometries where a large fraction of the gamma rays pass through the collimator to the detector at relatively large angles with respect to the normal, an experimental measurement will usually have to be made if accuracies approaching 0.1% are desired. This was done in work on the LANL standards as described in Sec. II.A.3. The term $[1 + (\mu_M^m/\mu_u^m)(\rho_M/\rho_u)]$ depends on the composition of the uranium compound or mixture, which must be known with reasonable accuracy if highly accurate enrichment measurements are desired. We note briefly here (from Refs. 1 and 5) that for matrix materials like oxygen, fluorine, and other elements with $Z < 30$ that $\mu_M^m/\mu_u^m \leq 0.1$. It is also true that for many uranium compounds such as UO_2, U_3O_8, etc., $\rho_M/\rho_u \sim 0.1 - 0.2$. Thus, the correction term $[1 + (\mu_M^m/\mu_u^m)(\rho_M/\rho_u)]$ rarely has values greater than 1.02 and, of course, if the sample is uranium metal the value is 1.0. As noted above, μ_u^m is slightly dependent on the isotopic distribution, or enrichment, of the uranium, so a correction for this should be made when striving for the greatest accuracy over a wide range of enrichment.

CLASSIFICATION

One other perturbation on the measurements not apparent in the simple one-dimensional expressions given here should be mentioned. If the densities of the standards and the unknowns to be measured are significantly different, there will be slight perturbations in the measured FEIRs because of $1/R^2$ effects. If one could use a point detector and a perfect conical collimator, there would be perfect compensation for those effects, but inasmuch as that is impossible with real detectors, there is some residual effect. This effect and several other minor ones are considered in detail in Matussek's report.[5]

A final correction, which should be considered here, is that for the interference to the 185.7-keV gamma rays of ^{235}U by low-intensity gamma rays of ~186-keV energy from ^{238}U daughter products. For the methods used to extract spectral peak areas in the work reported here, the effective rate of the interfering gamma rays is 0.32/s-g ^{238}U, while the emission rate for ^{235}U is $4.60 \cdot 10^4$/s-g ^{235}U. The factor by which the apparent measured enrichments should then be multiplied to compensate for this interference is

$$CF = 1 - \frac{\text{at.\% } ^{238}U}{\text{at.\% } ^{235}U} \cdot \frac{0.32}{4.6 \cdot 10^4} \quad . \tag{11}$$

For enrichments of 0.7, 2, 3, and 5% the CF values are very nearly 0.9990, 0.9997, 0.9998, and 0.9999, respectively. For enrichments above 5% the influence of this interference is clearly negligible. Again, the interference problem is dealt with in detail in Ref. 5.

2. Apparatus and Data Acquisition Procedures. Figure 24 is a schematic of the actual measurement geometry. Two different medium sized coaxial hyperpure germanium detectors were used during the course of the measurements. Both had a resolution of ~750-eV full width at half maximum (FWHM) at 122-keV. The associated electronics consisted of an Ortec 572 amplifier, a Canberra 8077 fast analog-to-digital converter (ADC), Canberra 8200 stabilizers, a Canberra Series 90 multichannel analyzer (MCA), and an Ortec 459 high-voltage power supply. The MCA was interfaced to a DEC PDP-11/23 computer for analyzing the spectral data. The amplifier was used with 3-μs time constants and pileup

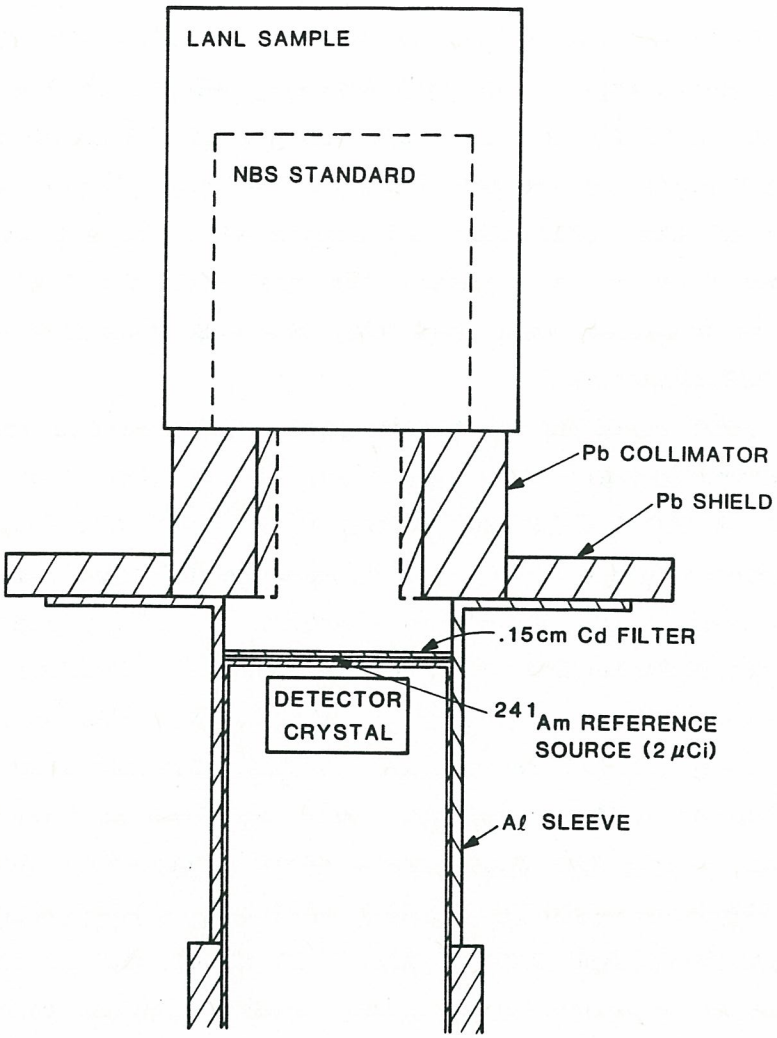

Fig. 24. A mechanical schematic of the actual counting arrangement used for gamma-ray measurements on both the LANL oxides and the NBS-969 certified reference standards.

rejection. The spectral data were accumulated in 1024 channels with an energy calibration of very nearly E(keV) ≈ (0.2 • Channel + 10), which was achieved by stabilizing the 59.5-keV full-energy peak from the ^{241}Am reference source at channel 248.0 and the 185.7-keV peak from the ^{235}U at channel 879.0.

The ^{241}Am reference source was about 2-μCi strength and was taped directly to the end cap of the detector with two-sided clear tape so that the detector saw a constant flux of the reference gamma rays save for the slow decay caused by the ~433 year ^{241}Am half-life. The ~0.15-cm-thick cadmium filter served to eliminate any interference by the 58.6-keV gamma ray from ^{235}U with the 59.5-keV reference gamma-ray full energy spectral peak, as well as to

generally lower deadtime and pileup losses by reducing the rate of useless lower-energy gamma and x rays. The cylindrically shaped lead collimator shown in Fig. 24 was 5.08 cm (2.00 in.) deep and was placed 1.9 cm above the detector end cap on a stand supported on the detector end cap flange to minimize any possible movement of the collimator and sample with respect to the detector. The collimator was 5.08 cm in diameter for use with the LANL standards and 3.8 cm (1.5 in.) in diameter when used with the NBS standards or for comparisons of LANL and NBS standards.

All spectra were recorded on floppy disks for analysis and possible reanalysis. The quantities extracted from the MCA spectra were the net full-energy peak areas of the 185-keV gamma ray of ^{235}U and the 59.5-keV gamma ray of the ^{241}Am reference source. As will be explained in Sec. II.A.3, the ratio of the two peak areas is independent of deadtime and pileup and is, therefore, proportional to the FEIR in Eqs. (6), (9), and (10). Because the peak area ratio is also independent of count time, all spectra were collected in true time for periods long enough, in general, to give the measured area ratio an estimated precision of 0.1% or better. With the 5.08-cm-diam collimator and the 2-μCi reference source the approximate times required to achieve a precision of 0.1% on the area ratio for various enrichments are plotted in Fig. 25. It is obvious that obtaining better than 0.1% precision on measurements of low-enriched uranium requires excessively long counting times. Figure 26 shows typical spectra from 91-, 52-, 10-, and 0.7%-enriched standards, demonstrating how the 185.7-keV peak decreases with respect to the reference peak as the enrichment decreases. The required time to reach 0.1% precision increases not only because of the decrease in the 185.7-keV net area, but because of the relative increase of the underlying Compton continuum, as described in Sec. II.A.3. The count times could have been reduced somewhat, perhaps by a factor of 2, by using a wider, shallower collimator (within the bounds allowed by the dimensions of the standards to be measured), which would have given increased count rates. That was not done because it was not desired to depart too far from an approximately linear geometry, while attempting to characterize standards with maximum accuracy.

3. Data Analysis Procedures. The fundamental information to be extracted from the MCA spectra is the net-full-energy peak areas of the 185.7-keV gamma ray of ^{235}U and the 59.5-keV gamma ray of the ^{241}Am reference source

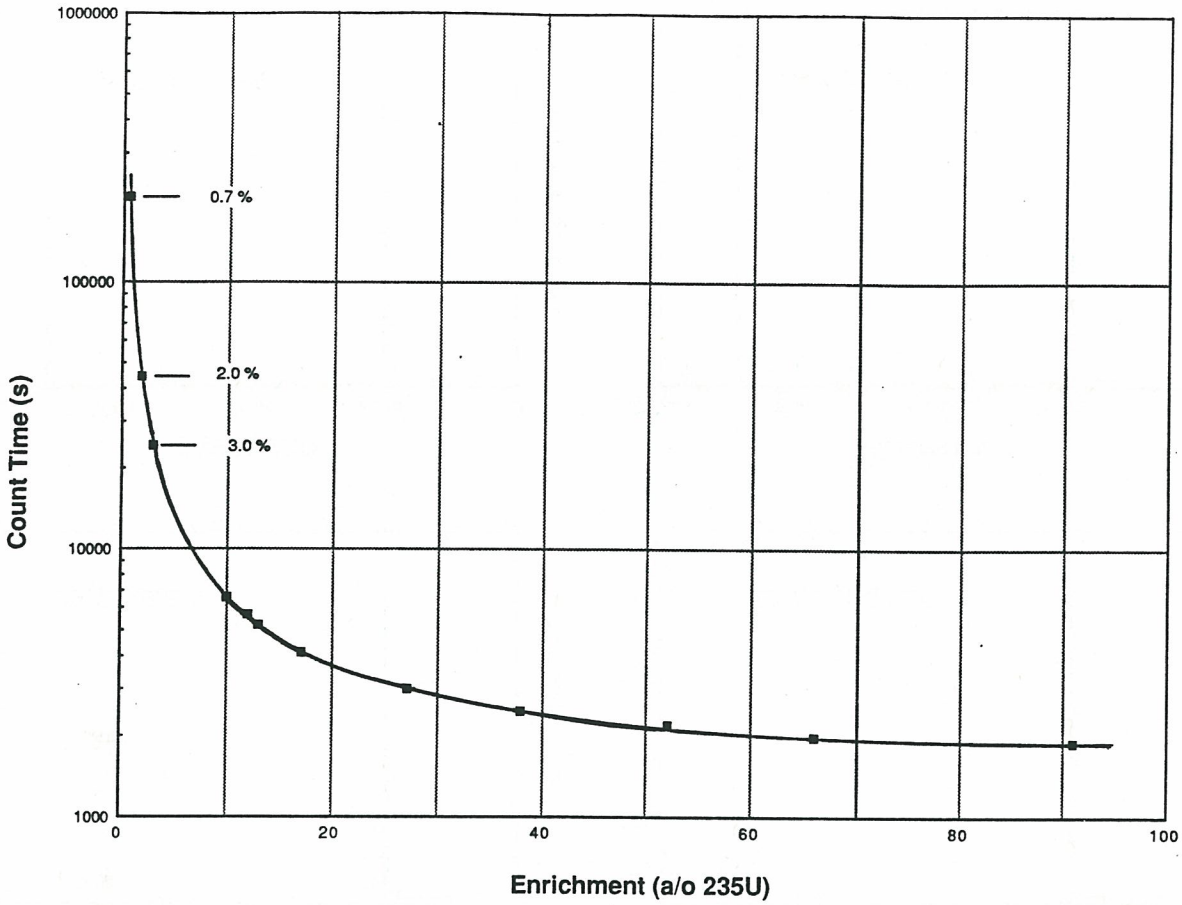

Fig. 25. A plot showing the count time in seconds required to obtain, with the LANL counting equipment used during the work reported herein, a 0.1% precision for the ^{235}U atom fractions as a function of enrichment.

along with the estimated precision of those net areas. It is important to obtaining unbiased enrichment measurements over a wide range of enrichment to extract the peak areas in a consistent, unbiased way as well. This assertion is, of course, true for most quantitative gamma-ray measurements, which cover wide ranges of activity in the nuclide(s) being measured. In the work described here, the areas were extracted from the spectra using region-of-interest (ROI) sums with a smoothed-step background subtraction algorithm. In this report, the word background will not have its traditional meaning but, following common usage in high-resolution gamma-ray spectroscopy, will refer to that part of the spectral continuum lying beneath the full-energy peak of interest that is not part of the peak. Although a straight-line approximation to that continuum is often used with good results, the real shape is definitely not straight, and it is thought that an effort to more closely approximate the

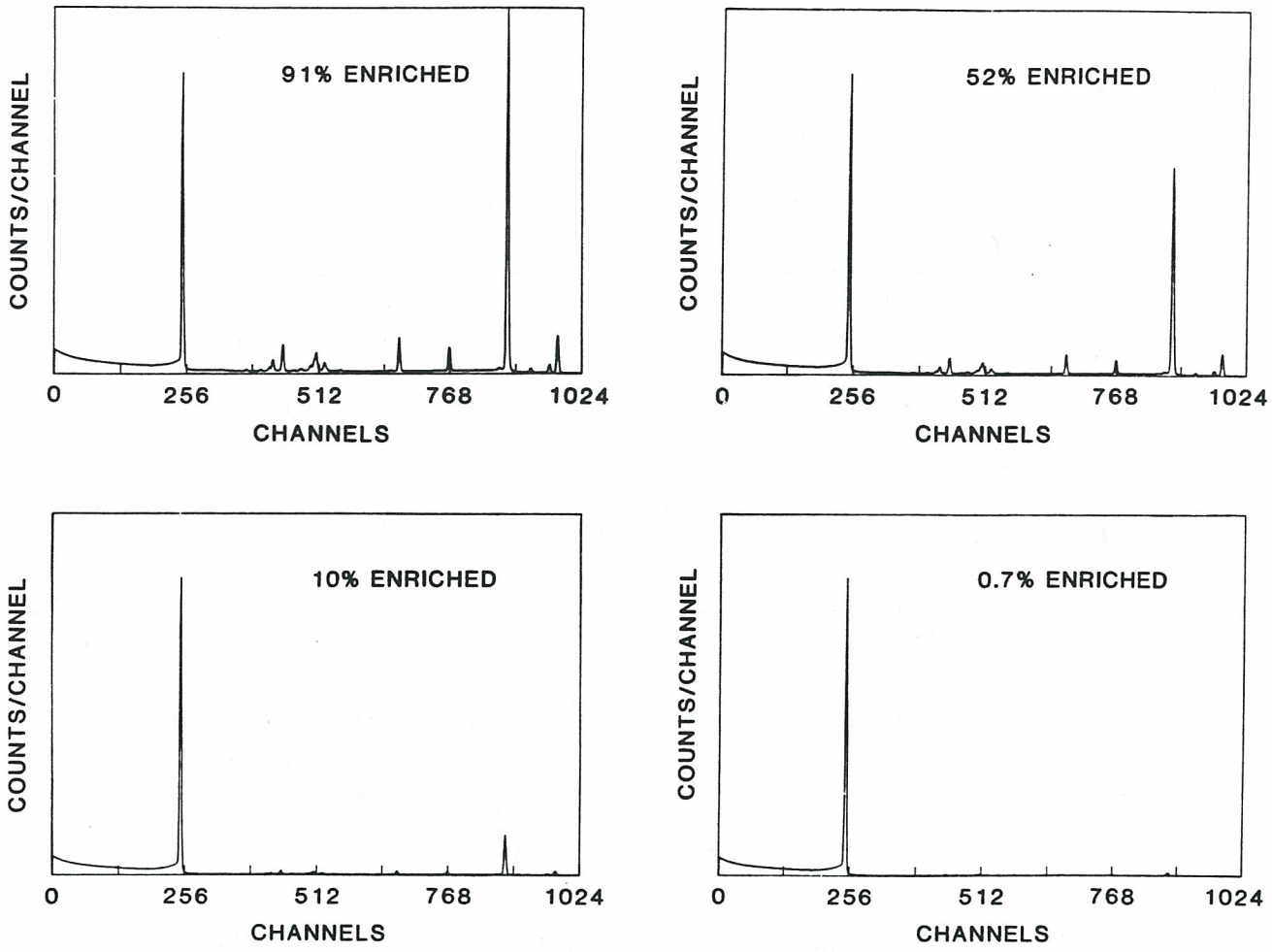

Fig. 26. High-resolution gamma-ray spectra from uranium oxide lots of four different enrichments with the LANL equipment used during the work reported herein.

real shape will give slightly more consistent results as the full-energy peak area changes greatly with respect to the area of the underlying continuum. The bulk of the underlying background continuum arises from the Compton scattering of higher-energy gamma rays or from the pileup of lower-energy gamma rays. That--usually smaller--part arising from the gamma rays generating the full-energy peak itself is caused by small-angle Compton scattering and incomplete charge collection of full-energy events. In terms of energy, this generates a relatively flat continuum with an abrupt cutoff at the gamma-ray energy that is a step function. The statistics of electron-hole pair formation, the processes of charge collection, and the system electronic noise smooth the background step and convert what would otherwise be a delta-function peak into

the familiar nearly Gaussian peak shape. Gunnink devised the original procedure to generate a smoothed-step background curve beneath single peaks or multiplets based on the overlying spectral shape. For overlapping peak multiplets, the procedure provides better results than the straight-line approximation, though as mentioned above the improvement for clean single peaks is less. Using the notation of Fig. 27, which shows the procedures for the straight-line

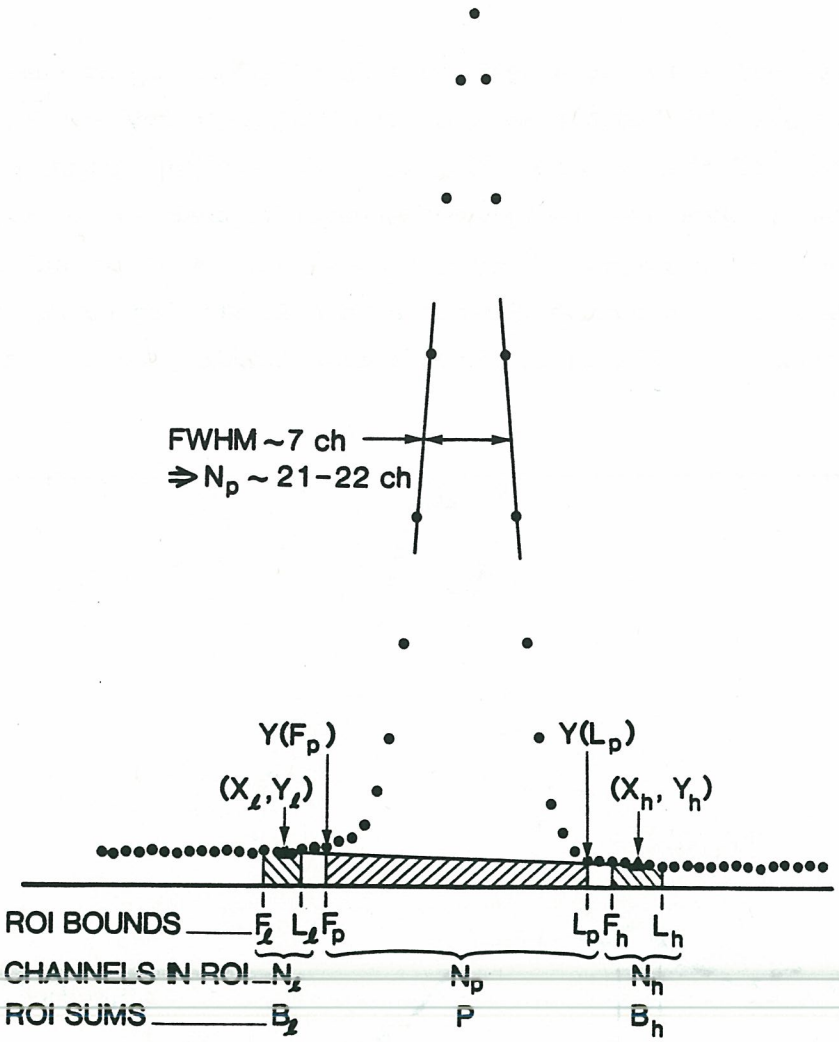

Fig. 27. ROI and associated parameters used in computing the net background-subtracted area of a full-energy peak and the estimated standard deviation thereof. X_ℓ, X_h are, respectively, the centers of low- and high-energy background ROIs; Y_ℓ, Y_h are, respectively, the average count/channel in the low- and high-energy background ROIs; $Y(F_p)$, $Y(L_p)$ are the ordinates of the background line at F_p and L_p, respectively; and $N_\ell = L_\ell - F_\ell + 1$, $N_p = L_p - F_p + 1$, $N_h = L_h - F_h + 1$.

methods, the expression for the background level at channel n is

$$B_n = Y_\ell - D \left\{ \left[\sum_{i=X_\ell+1}^{n} (y_i - Y_h) \right] / \left[\sum_{i=X_\ell+1}^{X_h} (y_i - Y_h) \right] \right\} . \qquad (12)$$

where $D = Y_\ell - Y_h$, and where $Y_\ell = B_\ell/N_\ell$ and $Y_h = B_h/N_h$. Y_h is subtracted from every channel because the Compton events from higher-energy gamma rays cannot influence the shape of the smoothed step for lower-energy gamma rays. Equation (12) is usable when the continuum beneath a peak or multiplet has a slightly negative or zero slope. The total background B to be subtracted from the peak ROI integral P to obtain the net area A is the sum of B_n over all the channels in the peak ROI. Figure 28 shows a logarithmic plot of a doublet with

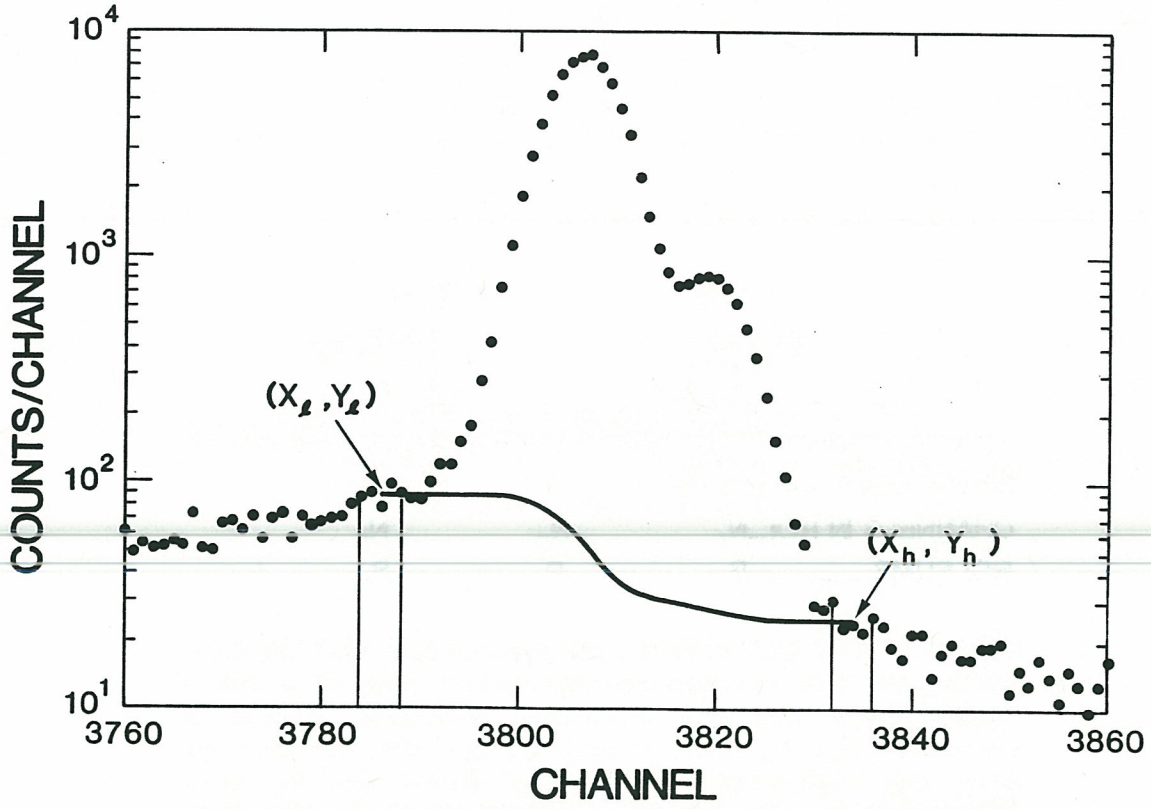

Fig. 28. A logarithmic display of an overlapping gamma-ray spectral doublet in which the background continuum has been estimated by the Gunnink smoothed-step algorithm.

the smoothed-step background generated by this algorithm. Note when using this method that N_ℓ and N_h should be odd numbers so that X_ℓ and X_h are integers.

A significant complication in using the smoothed-step procedure is that the expression for the precision of the net area becomes exceedingly complicated when derived from Eq. (12). Though such expressions have been derived, it is much simpler and almost as accurate to use the precision expression based on the straight-line approximation. Using the notation of Fig. 27 [same as Eq. (12)], the expression for the variance of B is

$$S^2(B) = (N_p/2)^2[C^2(B_h/N_h^2) + (2 - C)^2 (B_\ell/N_\ell^2)] \quad , \tag{13}$$

where $C = (F_p + L_p - 2X_\ell)/(X_h - X_\ell)$. For completeness, we note that if one wishes to use the straight-line approximation, the background is given by

$$B = [Y(F_p) + Y(L_p)](N_p/2) \quad . \tag{14}$$

Whether using the smoothed-step or straight-line method, the net peak area is given by

$$A = P - B \quad , \tag{15}$$

and in either case, the variance of the net area is given with sufficient accuracy by

$$S^2(A) = P + S^2(B) \quad . \tag{16}$$

As will be explained below, the ratio R of the 185.7-keV peak to the 59.5-keV peak is the quantity actually used in the enrichment expressions. We therefore note at this point that the estimated relative variance of R is given by

$$S_r^2(R) = S_r^2[A(185.7)] + S_r^2[A(59.5)] \quad ,$$

where by definition the relative variance S_r^2 of a quantity Q is given by

$$S_r^2(Q) = S^2(Q)/Q^2 \quad .$$

When accurate results over a wide range of count rate and area-to-background ratios are required, particular care must be used in setting up the ROI used in extracting the full-energy peak areas. Figure 29 shows in expanded form the 59.5- and 185.7-keV peaks with the ROIs used in the enrichment measurements reported here. As indicated, all the background ROIs were three channels (0.6 keV) wide, adequate to give good precision to the estimated backgrounds under the peaks without covering too wide a segment of sloping continuum. For both peaks, the peak ROI was set at 17 channels, just greater than 3 • FWHM of the 185.7-keV peak. Setting both peak ROIs equal helps in assuring the assumed equal loss to both peaks from pileup and deadtime. Because there is a little pileup-induced, high-energy tailing of the 185.7-keV peak (best seen in a logarithmic plot), the high-energy background ROI was centered at 189.4 keV, beyond the bulk of the tail. The 185.7-keV low-energy background ROI was centered at 181.2 keV on the low-energy side of the weak but interfering ^{235}U gamma ray at 182.7 keV. The 59.5-keV reference peak had negligible tailing and no nearby interfering gamma rays so the background ROIs were placed symmetrically with 1-channel gaps between them and the peak ROI. The smoothed-step background subtraction described above is particularly advantageous when background ROIs must be relatively far from the full-energy peak concerned, as in the case of the 185.7-keV peak.

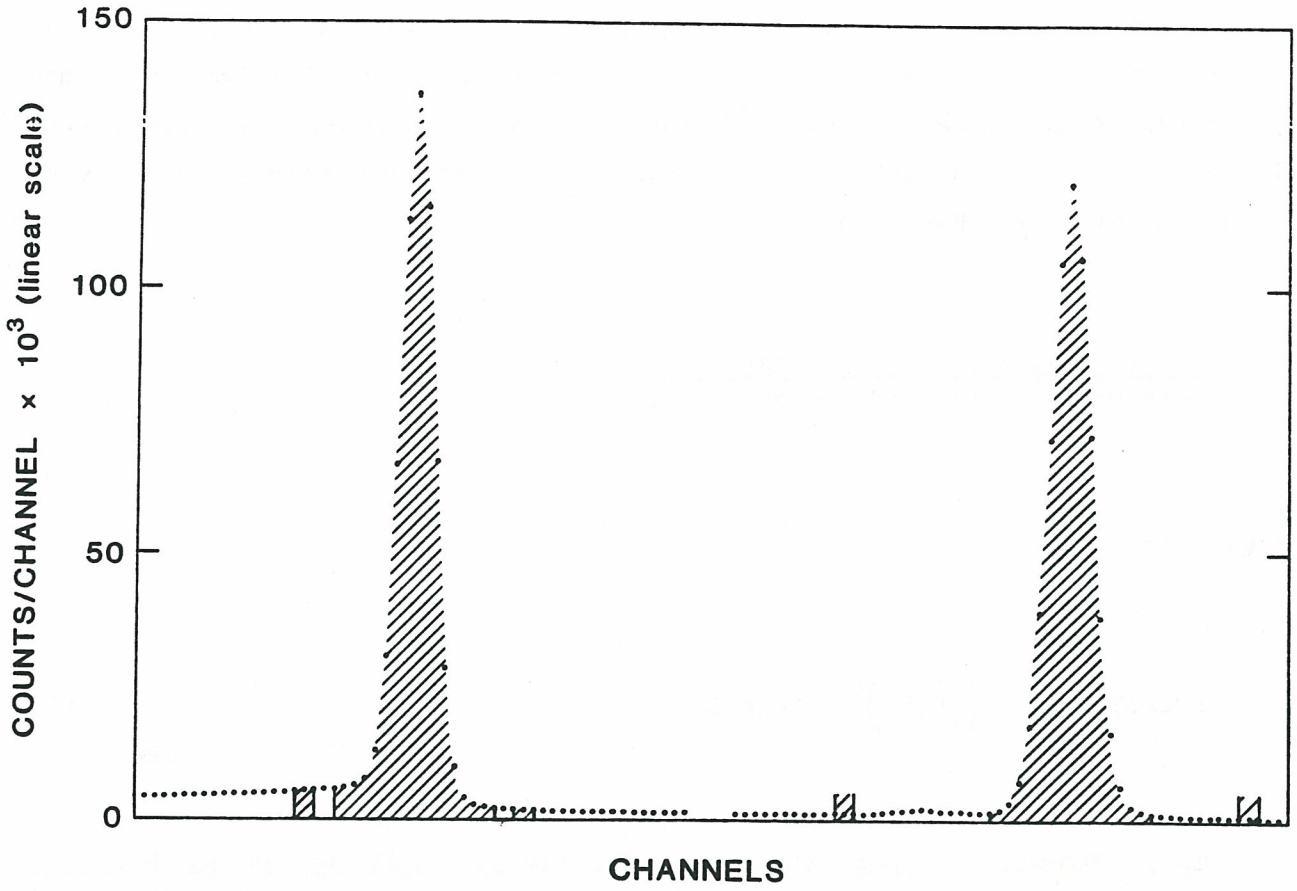

Fig. 29. Expanded spectral regions containing the ^{241}Am 59.5-keV gamma ray and the ^{235}U 185.7-keV gamma ray showing the ROIs used for full-energy peak area extraction during the work described in this report. Digital stabilization forces the 59.5-keV peak to remain centered at channel 248 and the 185.7-keV peak to remain centered at channel 879. The result is an energy calibration very close to E(keV) = 0.2 • Channel + 10.

Equation (10), the fundamental relationship between enrichment, measured quantities, and known parameters of the samples, includes the FEIR of the 185.7-keV gamma ray from the ^{235}U decay. The FEIR, of course, is greater than the raw signal rate, which is the net 185.7-keV peak area divided by the true acquisition time, because of the combined effects of pileup and deadtime in the electronics. There are various methods of correcting the raw rate to obtain the FEIR, but perhaps the most reliable for work such as reported herein is the use of a reference source, in this case ^{241}Am. This method, as is true of essentially all methods, depends on the fact that all the full-energy peaks in a spectrum lose almost the same fraction of net area because of the combined effects of deadtime and pileup. When the system is properly set up and other necessary conditions are met, the loss fractions can be made equal to

better than 0.1% over a wide range of count rate as has been done in the enrichment work reported here. It is easily shown that the FEIR(185.7) is proportional to the ratio of the ^{235}U peak and the ^{241}Am peak, A(185.7)/A(59.5). If f is the fraction lost to the effects of deadtime and pileup and T is the true time of data collection,

$$\frac{FEIR(185.7) \cdot (1 - f)}{FEIR(59.5) \cdot (1 - f)} = \frac{A(185.7)/T}{A(59.5)/T}$$

from which

$$FEIR(185.7) = \frac{A(185.7)}{A(59.5)} \cdot FEIR(59.5) \quad . \tag{17}$$

The constant of proportionality, FEIR(59.5), must indeed be constant, which is why the reference source is fastened tightly to the detector end cap, to ensure as far as is possible that the detector sees a constant flux of 59.5-keV gamma rays save only for the accurately predictable decay of the ^{241}Am. Though FEIR(59.5) could be determined with good accuracy, in this situation it is easier to absorb it into the constant term of Eq. (10). Thus, if we define the decay-corrected area ratio

$$R = [A(185.7)/A(59.5)] \cdot e^{-\lambda_{Am} t} \quad ,$$

where t is the time since determining FEIR (59.5), the fundamental relation becomes

$$R = \frac{K E T_p}{[1 + (\mu_M^m/\mu_u^m)(\rho_M/\rho_u)]} \quad , \tag{18}$$

where the $(1 - T_s)$ term has been dropped because $T_s = 0$ for all the work described here. Note that the decay corrections are small because every series of measurements reported here lasted no longer than 1 month, a small fraction of the 433-year ^{241}Am half-life.

During the characterization of the 19 cans of uranium oxide for possible use as standards, it was soon recognized, because of variations in the ^{235}U fractions among small samples from the same can that the average of the mass spectroscopic values, even though they were performed on 10 separate samples, might not correspond to the overall average value for the whole can. A major goal was to investigate the self-consistency of the whole set of possible standards when the observed counting data were interpreted with respect to the average mass spectroscopically determined enrichment. To do this, it seemed best to evaluate the constant K from Eq. (18), which should be a constant for the whole set of samples if all the factors are accurately known. The final expression used in the consistency study, therefore, is

$$K = \frac{R[1 + (\mu_M{}^m/\mu_u{}^m)(\rho_M/\rho_u)]}{E\ T_p} \quad . \tag{19}$$

Some comment on the factors in the above expression, and how their values were determined, is in order. The value of E used is that determined by the SAS statistics package and is very close to the unweighted average of all the mass spectrometer determinations, the results of which have been discussed in Sec. I of this report. Two procedures were used in determining the transmission factor T_p. For comparisons among the LANL cans whose bottoms varied in thickness by only about 0.003 cm, the expression $T_p = e^{-\mu\rho x}$ was used. Values ranged from 0.9728 to 0.9769, a variation of only 0.4%. Even though the absolute values were somewhat in error because of the wide-beam counting geometry, the ratios of the values are very adequately correct. For comparisons between NBS SRM-969 and the LANL cans of oxide, however, there is an ~4% difference in T_p values, too much for the simple estimate and direct measurements were therefore required. Those measurements were made using one of the highly enriched LANL standards as source and actually measuring the transmissions of discs of

metal nearly equivalent to the bottoms of the two sets of standards in the same counting arrangement used for acquiring the enrichment data. Slight corrections were then made for the known slight variations in the bottom thicknesses within the two sets. The LANL cans have steel bottoms ~0.02-cm thick with T_p ~ 0.976, while the NBS SRM-969 containers have aluminum bottoms ~0.2-cm thick with T_p ~0.934.

The composition factor $[1 + (\mu_M^m/\mu_u^m)(\rho_M/\rho_u)]$ is computed from measured and tablulated values of the required quantities. The ratio ρ_M/ρ_u is derived from the average uranium fractions given in Table V using the relation $\rho_M/\rho_u = (1 - \%U)/\%U$. For the ratio μ_M^m/μ_u^m, the matrix was assumed to be pure oxygen and the tabulated value for oxygen at 185.7 keV was used. The value of μ_u^m was adjusted according to the known approximate isotopic distribution of the various standards. Assuming that tabulated values are for normal uranium, which is 99.27% ^{238}U, the adjustment was made by multiplying the tabulated value by 238.029 and dividing by the known approximate average atomic masses for the different standards. This procedure is in accord with Eq. (1), which shows that the mass-attenuation coefficients are inversely proportional to the average atomic mass of an elemental sample. Though the adjustment makes only ~0.01% difference in the value of the composition factor and is, thus, only marginally necessary it was done, if for no other reason, to recognize that the attenuation coefficients are not utterly constant for uranium samples of widely different isotopic distributions.

B. Measurement Results

The work described in this report had two major goals, to characterize a consistent wide-range set of enrichment standards and to explore the limits of precision and accuracy of gamma-ray enrichment measurements. In the course of trying to achieve those goals, enrichment measurement data were obtained in four different categories as follows:

(1) Comparative measurements among the standards of NBS SRM-969, all of which have enrichments of $\leq$4.5%.

(2) Comparative measurements between SRM-969 and some of the LANL standards of $\leq$10% enrichment.

(3) Comparative measurements among the LANL standards of $\leq$3% enrichment.

(4) Comparative measurements among the LANL standards of $\geq$10% enrichment.

The measurements of the four categories will be discussed separately to be

CLASSIFICATION

followed finally by some discussion and observations on the precisions and accuracies observed and on the limitations and main sources of error in such measurements.

1. **Comparative Measurements on NBS SRM-969.** Because of the high confidence in the stated parameters of these very carefully fabricated and certified standards, they were carefully counted before work began on the LANL materials. This procedure allowed the stability and potential accuracy of the whole experimental arrangement to be evaluated before starting work on relative "unknowns." These standards were counted on a collimator 3.8 cm (1.5 in.) in diameter by 5.08 cm (2.00 in.) deep, rather than the 5.08-cm diam one used for comparisons among the LANL standards. This diameter was used because of the somewhat smaller diameter of the containers and the necessity to maintain an infinite thickness in all parts of the standards viewed by the detector. Otherwise the counting geometries were the same. Because of the somewhat smaller collimater, counting times were about 30% longer to achieve the same precision than for the larger collimater for which the count times as a function of enrichment are given in Fig. 25. Counts were made over a month with at least three and as many as seven counts being made on each standard. To illustrate how difficult it is to achieve high precision on samples of very low enrichment, the four separate counts on the 0.3%-enriched standard took a total of 1 110 000 s (13.1 days) to obtain an estimated 0.08% precision on the average value of K. For each separate count on a standard, the value of K was computed according to Eq. (19). The estimated precision of K was taken as the estimated precision of the measured area ratio, R, in Eq. 19. Figure 30 is a plot of the deviations of all the observed K values from the average of the 4.5%-enriched values. In all cases, the values of R were corrected for the interference from the ^{238}U daughters and for the decay of the ^{241}Am reference source. The average values for each standard are shown by the cross on the right of the group of individual values for that standard.

A few things are worth noting. The spread of the averages is only about ±0.1% with estimated 1-standard-deviation error bars ranging from ~0.03% for the 4.5% standard to ~0.08% for the 0.3% standard. This represents very good consistency between the certified parameters and the measured quantities, giving confidence that measurements of similar materials could be made with

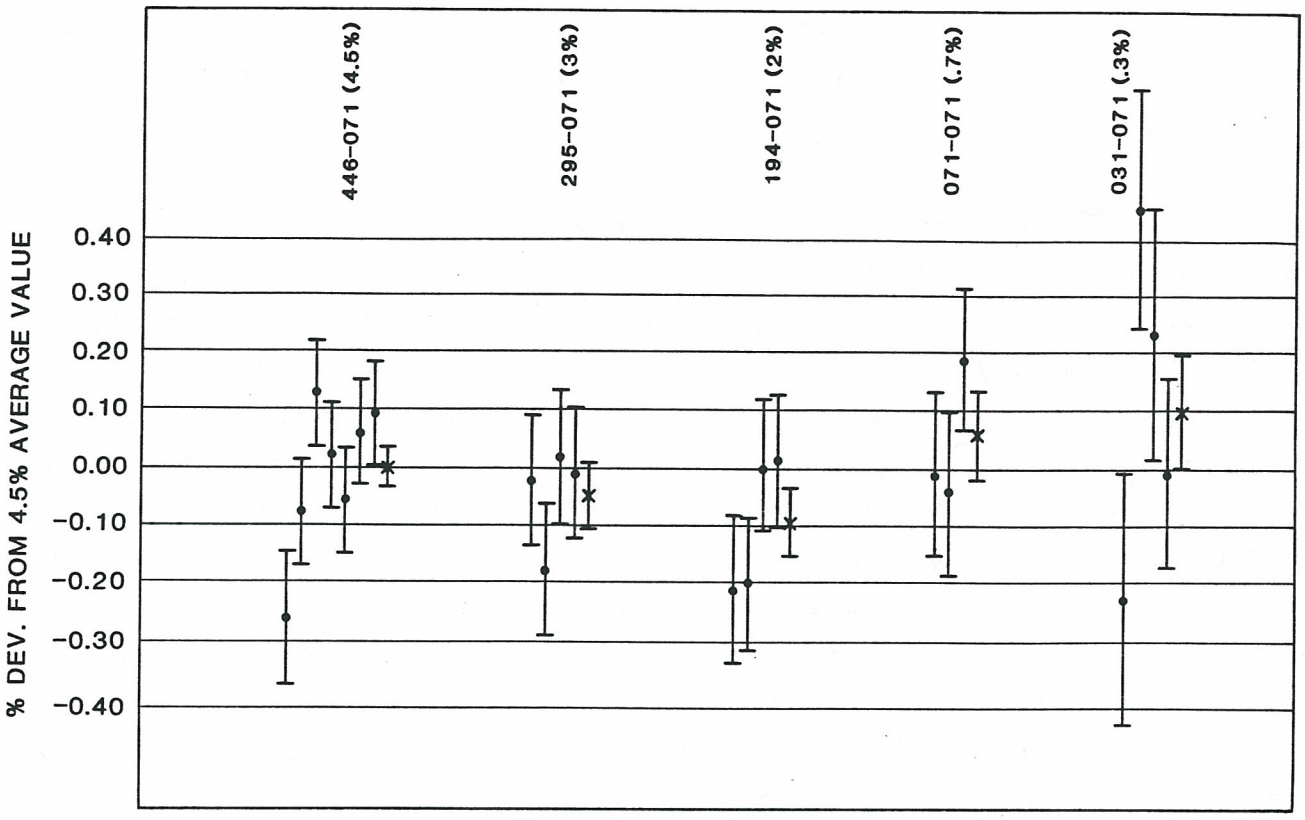

Fig. 30. A comparison of the results of careful gamma-ray counting of the NBS SRM-969 enrichment standards. The quantity calculated is the total corrected count rate divided by the accepted enrichment [the K value of Eq. (19) discussed in the text]. Results are presented as percentage deviations from the average value of the 4.5%-enriched standard. If both counting and the accepted enrichment values were without error, all points would lie along the 0.0 line.

respect to these standards with measurement biases of $\leq$0.1%. With the precisions of Fig. 30, it is impossible to tell whether a real trend exists among the averages, though the K values do seem to systematically decrease and then increase toward smaller values of enrichment. It is interesting to observe (though it may not prove anything) that a similar apparent trend exists within results, published in Ref. 5, of similar though not quite so precise measurements on SRM NBS-969. The scatter of the points for the individual standards indicates that the stability of the measurement system over a significant time is very good, though not perfect. The probabilities for the observed scatter in the five cases to occur randomly are 14%, 61%, 35%, 41%, and 12%, in descending order from the 4.5% standard. If the spread of the measurements was governed only by the purely random processes of photon emission, it would be

CLASSIFICATION

expected that the average probability would be about 50%. The fact that the average is only 33% indicates time-dependent changes of perhaps a few hundredths of a percent occurring during the month occupied by the measurements. Such changes could occur because of slight changes of position of the collimator with respect to the detector, because of even smaller changes in position of the reference source with respect to the detector crystal, or even because of slight changes in the detector efficiency. In the present case, it was also found after the data were all acquired that the detector used had a significant microphonic sensitivity so that the rather high level of room noise caused the amplifier base line to break up occasionally, creating yet another possible source of nonrandom error.

Other possible sources of nonrandom error are negligible among the five standards of NBS SRM-969. The containers are so uniform and the composition of the oxides so close to stoichiometric U_3O_8 that the container and composition terms of Eq. (19) did not vary by so much as 0.01%. The bulk densities are also sufficiently similar that $1/R^2$ effects are also negligible.

2. Comparisons Between SRM-969 and Some LANL Standards. A series of comparative measurements were made between the 4.5, 3.0, and 2.0% standards of SRM-969 and LANL standards of 10.2, 3.1, 2.0, and 0.73%. At the time of the measurements, there was no doubt about the available ^{235}U enrichment values for any of the LANL standards and the motivation for the measurements was primarily to demonstrate the ability to make corrections for significantly different container transmissions, the T_p of Eq. (19). The container bottoms of SRM-969 are 0.20-cm-thick aluminum with a density of 2.70 g/cm^3, whereas the container bottoms of the LANL standards are 0.021-cm-thick steel with a density of 7.86 g/cm^3. The roughly estimated transmissions are 97% and 93% respectively, a difference of 4% for which corrections must be made to better than 0.1% if SRM-969 is to be used in calibrating for 0.1%-accurate measurements of samples similar to the LANL standards.

All the comparative data were acquired with the 3.8-cm-diam by 5.1-cm-deep collimator appropriate for the SRM-969 standards. When the T_p factors were estimated from the simple expression $T_p = \exp-(\mu\rho t)$, the K values of the LANL standards were biased about 0.3% high relative to the SRM-969 K values, indicating the need for direct, broad-beam T_p measurements in the actual collimator geometry. Those measurements were done as described in Sec. II.A using a can

of highly enriched oxide to obtain better precision in a reasonabletime. The change was mostly in the transmission of the SRM-969 standards, which because of their lower transmission had the greatest error in the estimated value. Figure 31 gives the K values obtained with the measured transmissions and with the appropriate corrections for the influence of the ^{238}U daughters. As seen, the average difference in values between the SRM-969 and LANL standards is ~0.08%--good agreement considering that the estimated precision of the ratio of the two T_p values is 0.06%.

The conclusion of this exercise is that highly accurate enrichment measurements can be made in which the calibration standards and unknowns are in packages with significantly different T_p values, but that the corrections for

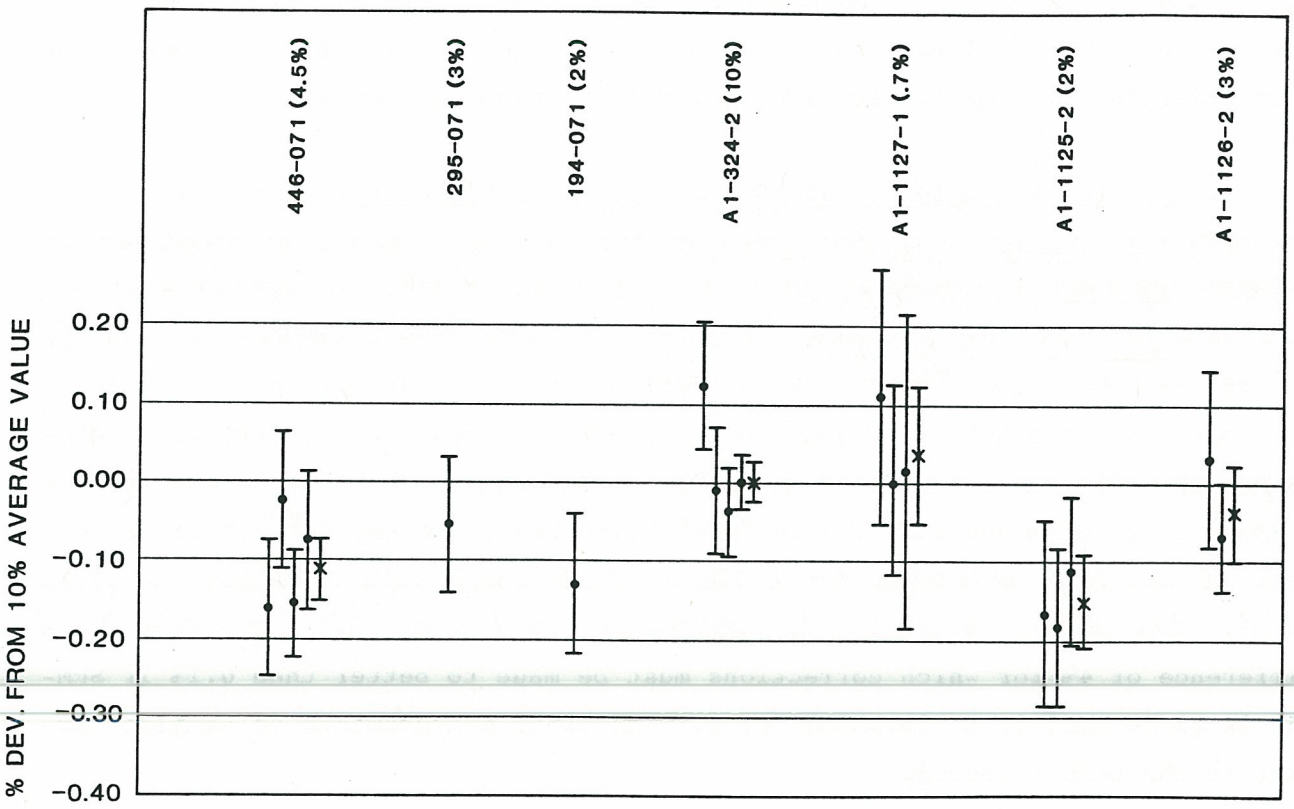

Fig. 31. Results of comparative counting between some of the NBS SRM-969 enrichment standards and some of the LANL working standards in the same enrichment range. The quantity calculated is the total corrected count rate divided by the accepted enrichment [the K value of Eq. (19) as discussed in the text]. Results are presented as percentage deviations from the average value from the 10%-enriched standard. If both counting and the accepted enrichment values were without error, all points would lie along the 0.0 line.

those differences will probably have to involve a direct measurement. Those extra measurements can greatly increase the amount of work involved. To make this more explicit, the expression for the enrichment of an unknown in terms of the enrichment of a single calibration standard is

$$E_u = \left(\frac{R_u F_u T_u}{R_s F_s T_s} \right) E_s \quad , \tag{20}$$

where E = the enrichment,
R = the area ratio of Eq. (19),
T = the package transmission of Eq. (19),
F = the composition factor of Eq. (19), and where
subscript u = values relating to unknowns,
subscript s = values relating to calibration standard.

It is now clear that R_u, R_s, T_u, and T_s must all be measured with precision better than that desired for E_u, in fact with precisions twice as good as that desired for E_u, if all quantities are measured with equal precision. It is also clear, though it has nothing to do with the T_p factor, that the compositions of both standards and unknowns must be known well enough to compute the ratio of the composition factors F_u/F_s with accuracy considerably better than that required for E_u.

3. Comparison Among LANL Standards of ≤3% Enrichment. The set of 19 LANL standards falls naturally into two groups, those of ≤3% enrichment and those of ≥10% enrichment, and results from the two groups will be discussed separately, even though data from both groups were sometimes acquired in the same measurement series. Two full sets of measurements were made on the eight standards in the lower-enriched group. The two sets were acquired about 4 months apart and with different detectors, but were tied together by normalizing all results to the K values obtained from the periodic measurement of the 17% standard. The 17% standard was used as a stability check sample during all sets of measurements because it was the highest enriched standard that could be kept

continually at the Laboratory, and thus could give the best precision in a reasonable time of those regularly available. The results of the two series of measurements are given in Fig. 32, the format being the same as for Figs. 30 and 31. The precisions of the individual points range between 0.05 and 0.1%, the better values corresponding to the higher enrichments. Reference to Fig. 25 emphasizes the nontrivial effort in obtaining better than 0.1% precision on low-enrichment samples. Most counts were for about 1 day (80 000 to 90 000 s), with some occupying entire weekends. The plotted points for the 0.7% standards are all averages of three or four counts, whereas the points for the higher enrichments generally come from a single count. The agreement between the two sets of measurements is good in six of the eight cases. In the other two cases, the separations of the points are so great that either very low-probability events occurred or some nonrandom effect perturbed one or both

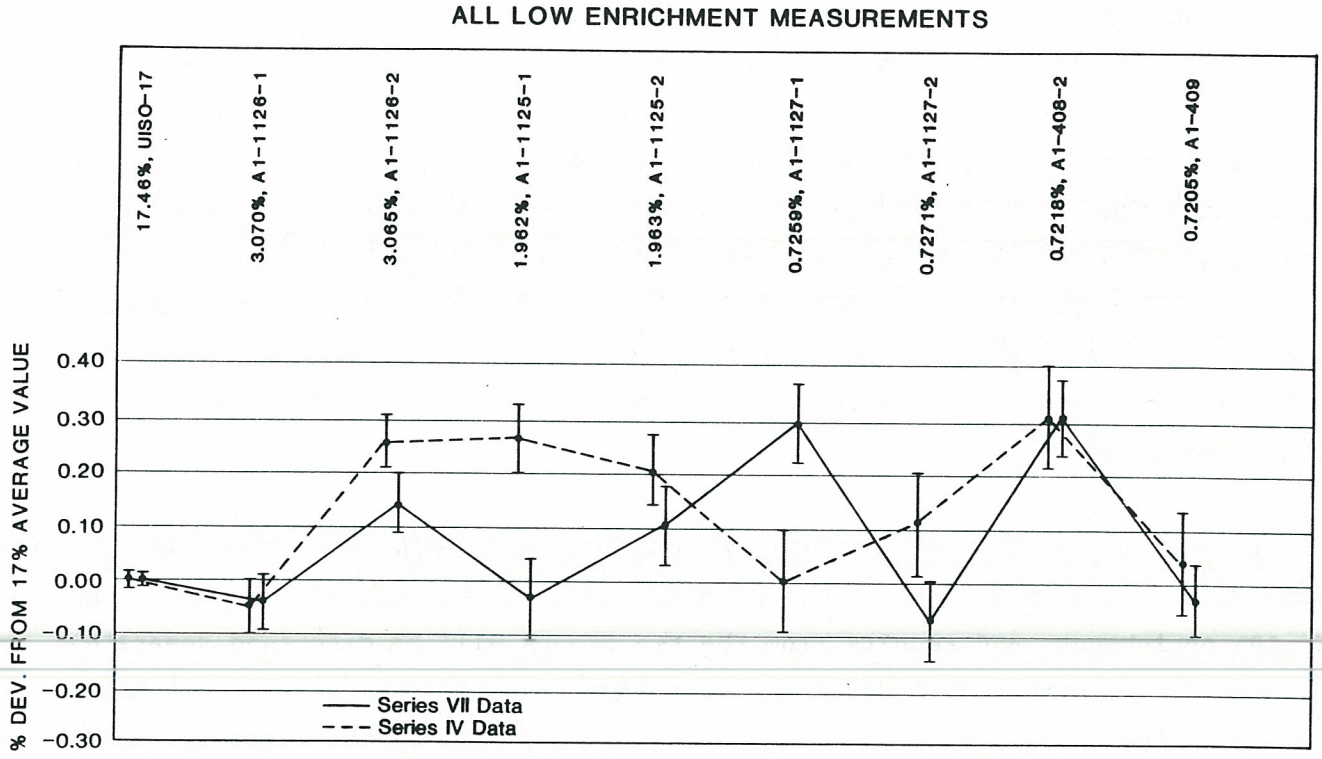

Fig. 32. Results of comparative counting among the LANL standards of $\lesssim$3% enrichment. The quantity calculated is the total corrected count rate divided by the accepted enrichment [the K value of Eq. (19) as discussed in the text]. Results are presented as percentage deviations from the average value from the 17%-enriched LANL standard that was used as a long-term stability check. If both counting and the accepted enrichment values were without error, all points would lie along the 0.0 line.

CLASSIFICATION

of the measurements to the combined extent of 0.1 to 0.2%. It is, nonetheless, a good demonstration of reproducible results over a long period of time including changes of detector and electronics.

Another set of comparisons is of interest. Among the 19 cans of uranium oxide characterized are 4 pairs, apparently from the same lots of oxide. They are:

(1) A1-324-1 and A1-324-2 at 10.20%;

(2) A1-1126-1 and A1-1126-2 at 3.06%;

(3) A1-1125-1 and A1-1125-2 at 1.96%;

(5) A1-1127-1 and A1-1127-2 at 0.726%.

As discussed in Sec. I, for more than half of the 19 cans of uranium oxide there was a real and surprisingly large variation in the mass spectrometrically measured isotopic distributions among the 10, ~30-mg samples dissolved for analysis from each can. As seen in Figs. 2 through 20, sample-to-sample variations of up to 2% relative exist in the ^{235}U atomic fractions found. If the variations are essentially a microscopic phenomenon, then it would be expected that the average over 10 samples representing 300 mg of oxide would give a result nearer to the true average value. This expectation seems to be true, for the averages in every case give better consistency when compared with gamma-ray counting than any of the extreme values, though deviations from the norm of several tenths of a percent still exist. It would then also be expected that the gamma-ray counts, which sample ~30 g of oxide should be an even better measure of average enrichment. This expectation too seems true, for the counting data on all the pairs listed above indicate that the enrichment of both members of each pair is the same within 0.1%. For the 10.2% pair, this result is no surprise as the mass spectrometer data were very consistent, but in the case of the other three pairs, wherein the scatter of the 10 values was much greater, the average mass spectrometer values between members of a pair varied by 0.17% in two of three cases. For these reasons, it is believed that the adjusted values given for the ^{235}U atom fractions of the items on the secondary standard list, based on gamma-ray spectrometry, are closer to the real averages over the mass and volume of the standards, than are the averages of the 10 mass spectrometer values.

4. Comparison Among LANL Standards of ≥10% Enrichment. Three full sets of measurements were made on the 11 standards in the higher-enriched group.

The first series was made during October 1985, the second during November 1985, and the third between January 8 and February 11, 1986. As with the lower-enrichment standards, two different detectors were used, the collimater assembly was dismantled and reassembled, and changes in electronics were made during the course of the work. Also, as with the lower-enrichment set, the three sets of data were tied together by normalizing all the results to the average K values obtained from the frequent measurement of the 17% standard, which served as a stability check sample throughout. The results of the three series of measurements are given in Fig. 33. As seen there, the precision of the plotted points varies from about 0.02 to 0.05%, and some of the points represent averages of more than one count. The consistency between the three sets of values is generally very good, though in a few cases the scatter of the three points when compared with the estimated errors has a fairly low probability, indicating that nonrandom drifts or changes of up to 0.05% may have

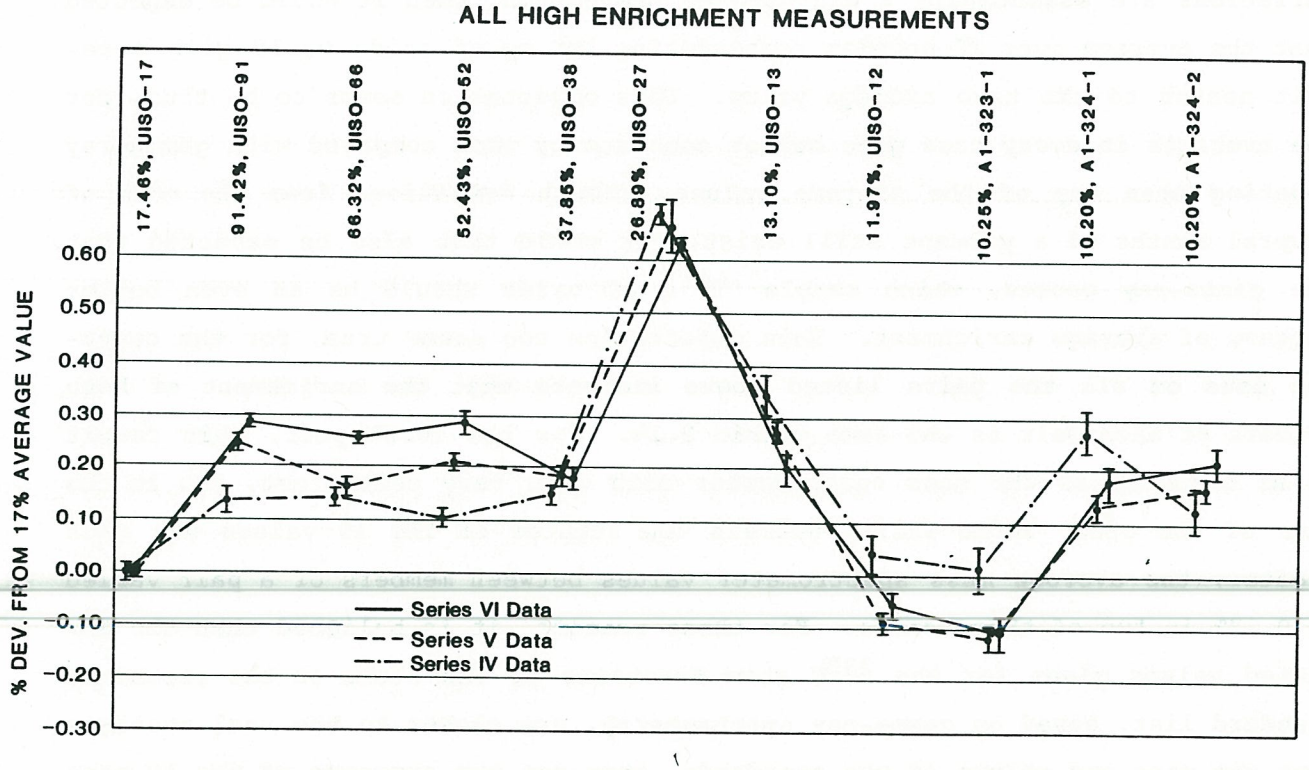

Fig. 33. Results of comparative counting among the LANL standards of ≥10% enrichment. The quantity calculated is the total corrected count rate divided by the accepted enrichment [the K value of Eq. (19) as discussed in the text]. Results are presented as percentage deviations from the average value from the 17%-enriched LANL standard that was used as a long-term stability check. If both counting and the accepted enrichment values were without error, all points would lie along the 0.0 line.

occurred. The possible causes for such nonrandom error are the same as those mentioned above for the comparisons among the lower-enriched group. The results still are a solid demonstration of reproducible results at the 0.1% level over a long period of time including changes of detector and electronics.

As a specific example of stability, Fig. 34 gives the deviations of the K values from their average for 14 measurements of 10 000 s each on the 17%-enriched stability check standard during a period of 24 days. The points all have estimated RSDs of 0.064% and the sample RSD of the 14 values is 0.072%. This is gratifyingly good agreement though the reduced chi-square value is 1.23, with a probability of only 25% to occur on a purely random basis, indicating that nonrandom effects of a few hundredths of a percent may have been present.

As mentioned above in the discussion of the measurements on the lower-enriched standards, the variations in ^{235}U atomic fraction observed within many

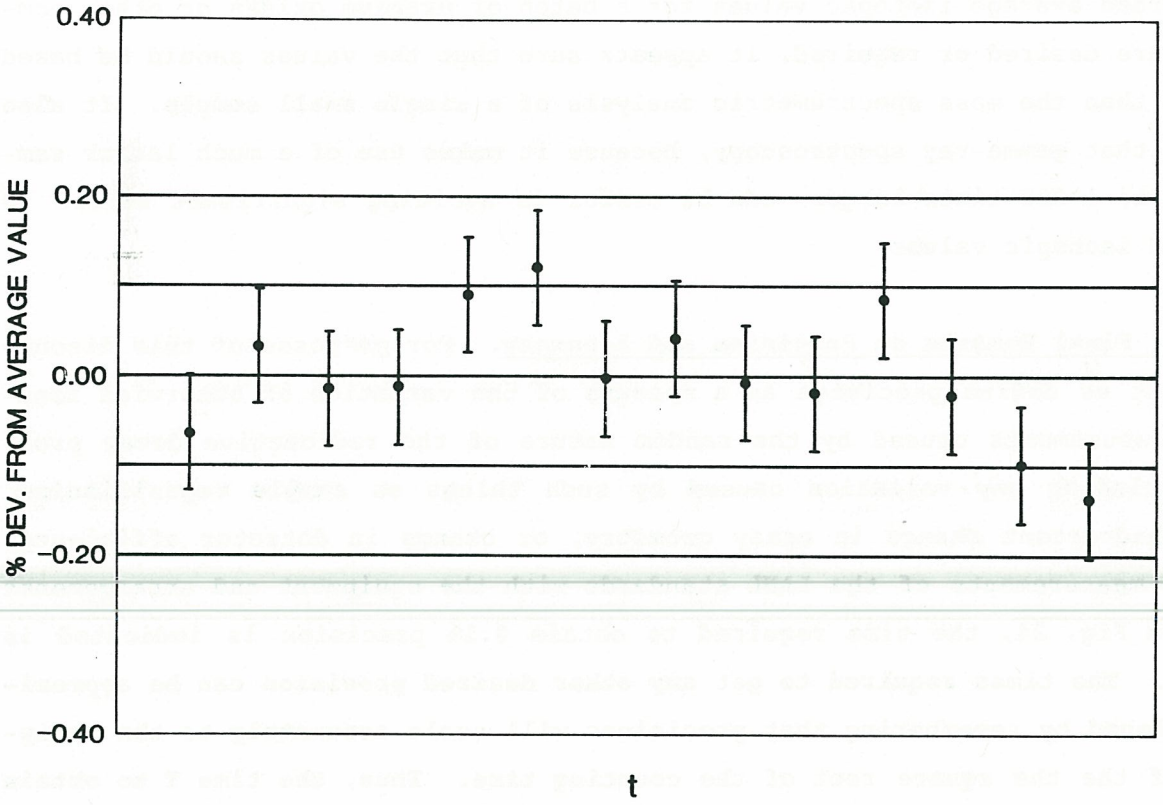

Fig 34. Long-term stability data from the LANL 17%-enrichment standard. It presents the total corrected count rate and the estimated precisions for 14 counts spread over 24 days. The data are presented as percentage deviations from the average of all 14 values.

of the standards seems related to the small (~30 mg) sample dissolved for mass spectroscopy. The variation seems to shrink as the sample size increases. To confirm this, the higher-enriched standards were counted in the usual bottom-side-down configuration, again in the bottom-side-up position, and yet again in some cases after having been thoroughly shaken. The result is independent gamma-ray measurements on essentially two or three different ~30-g samples. In no case did any of the measurements of the same can differ by more than 0.1%, with estimated relative RSDs usually $\leq$0.05%, even though mass spectrometer values on the small samples from the same can differed by as much as 2%.

Whether the variation of isotopic distribution among small samples observed for some of the 19 cans of uranium oxide is common among processed uranium compounds is not known for a certainty. However, the materials in those 19 cans of oxide came from at least three different sources, and such variations were noted in some cans from all of the different sources, thus raising a strong suspicion that such isotopic heterogeneity may be quite widespread. If accurate average isotopic values for a batch of uranium oxides or other compounds are desired or required, it appears sure that the values should be based on more than the mass spectrometric analysis of a single small sample. It also appears that gamma-ray spectroscopy, because it makes use of a much larger sample--up to 1 000 times larger--can be useful in avoiding significant errors in assigned isotopic values.

5. Final Remarks on Precision and Accuracy. For purposes of this discussion, let us define precision as a measure of the variation of otherwise identical measurements caused by the random nature of the radioactive decay process, excluding any variation caused by such things as sample repositioning, other inadvertent change in assay geometry, or change in detector efficiency. For the measurements of the LANL standards with the equipment and arrangements shown in Fig. 24, the time required to obtain 0.1% precision is indicated in Fig. 25. The times required to get any other desired precision can be approximately found by remembering that precisions will scale accurately as the reciprocal of the the square root of the counting time. Thus, the time T to obtain for a given enrichment, any desired %RSD is given by

$$T = \left(\frac{0.1}{\%RSD}\right)^2 \cdot t(0.1\%) \quad , \tag{21}$$

where t(0.1%) is the time to obtain 0.1% precision obtained from Fig. 25. The precision of a given determination is, of course, determined from the RSDs of the two net-full-energy peak areas from the relation %RSD(E) = {%RSD[A(185.7)] + %RSD[A(59.5)]}$^{1/2}$. Obviously, when possible, percision may be improved by longer counts. Also, if sample sizes permit, larger collimators can give increased count rates and therefore better precision for a fixed time. It should also be remembered that if a measurement of the quantity T_p is required that the precision of that quantity must be folded into the precision of the enrichment result.

Accuracy is a term that has suffered so many usages that its usefulness as a word has almost been destroyed, unless it is defined with every use. Accordingly, we use accuracy here in the sense of "nearness to truth." A measurement that is very accurate will therefore have both to be highly precise and to suffer very low biases, where the term biases includes all those effects that cause relatively constant additive or multiplicative measurement errors for a given class of unknowns or for a particular set of apparatus. Biases, as we use the term here, can include effects that are constant in time or that may vary slowly in time and thus include what some writers may call "long-term" precision. We prefer the term bias, because such effects on the results of a given day or for a number of days is likely to be rather constant.

Among those biases that might be of relatively large magnitude, a major category includes those arising from improperly adjusted equipment or equipment suffering slow changes in some important operating parameters. Improperly adjusted equipment is, of course, a source of difficulty that can be avoided with care and well-trained measurement equipment operators. Among relatively long-term effects arising within the measurement equipment itself are those caused by very small changes of position of the reference source relative to the detector, small changes of position of the collimator relative to the detector, and by time-dependent (and possibly energy-dependent) changes of the full-energy interaction efficiency of the detector itself. Some effects may have their origins outside the equipment itself. These include the usually low-frequency signals induced in germanium detectors by virtue of their extremely microphonic properties in an acoustically noisy environment, and the usually higher-frequency signals picked up from many possible sources of electromagnetic noise. Some possible biases, though their magnitudes will usually be small, are caused

by lack of exact knowledge of the composition of the samples themselves. Examples are errors in the thickness or density or composition of the sample container when the package transmission T_p is being estimated. Another example would be error in the chemical composition of the uranium compound being measured, which causes error in the correction term $[1 + (\mu_M^m/\mu_u^m)(\rho_M/\rho_u)]$.

The possibility of those problems mentioned makes imperative the use of a good measurement control program for measurement systems doing routine measurements over long periods. Certainly, daily checks are required at sufficiently high precision to detect the presence of biases at an adequately low level. The nature of an adequate measurement control program is not part of this report, nor is the nature of a good instrument calibration plan, but both should be considered most carefully if consistently accurate measurements of uranium enrichment are desired.

In conclusion, it seems that one or more of the bias effects mentioned above (as well as possible others not yet recognized) are usually present at levels of a few hundredths of a percent so that it is difficult to hold cumulative bias effects to levels below 0.1% without the most strenuous efforts. It is, therefore, even more difficult to keep the RSD distribution of a set of measurements to $\leq$0.1%, particularly when items of differing enrichment, composition, and especially packaging are being measured. To end on a positive note, it appears that with reasonable skill and care, comparisons among items of well-known composition, nearly identical and well-known packaging, and higher though widely varying enrichments can indeed be made with accuracies very near the 0.1% level in reasonable counting times. Indeed, at this time (autumn 1986), 0.1% still seems to be the limit of "practical capability" for the accuracy of gamma-spectrometric measurements of uranium enrichment.

REFERENCES

1. T. D. Reilly, R. B. Walton, and J. L. Parker, "The 'Enrichment Meter'-- A Simple Method for Measuring Isotopic Enrichment," in Los Alamos Scientific Laboratory report LA-4605-MS (January 1971), pp. 19-21.

2. L. A. Kull and R. O. Ginaven, "Guidelines for Gamma-Ray Spectroscopy Measurements of ^{235}U Enrichment," Brookhaven National Laboratory report BNL-50414 (1974).

CLASSIFICATION

3. T. D. Reilly, "Gamma-Ray Measurements for Uranium Enrichment Standards," in Measurement Technology for Safeguards and Materials Control, (NBS Special Publication 582, National Bureau of Standards, 1980) T. R. Canada and B. Stephen Carpenter, Eds., Proc. ANS Topical Meeting, Kiawah Island, South Carolina, November 26-30, 1979, pp. 103-110.

4. H. Ottmar, "Note on the Contribution of ^{238}U Daughter Products to the 185-keV Gamma-Ray Intensity Observed for LWR Fuels," Private Communication, 07.01.03p09A, February 1980.

5. P. Matussek, "Accurate Determination of the ^{235}U Isotope Abundance by Gamma Spectrometry, A User's Manual for the Certified Reference Material EC-NRM-171/NBS-SRM-969," Kernforschungszentrum Karlsruhe report KfK 3752, Karlsruhe, Federal Republic of Germany (May 1985).

6. J. H. Hubbell, "Photon Cross Sections, Attenuation Coefficients, and Energy Absorption Coefficients from 10-keV to 100-GeV," National Bureau of Standards report NSRDS-NBS 29 (1969).

CLASSIFICATION

APPENDIX

ALL LANL AND NBL VALUES OF ATOM PERCENT ^{235}U

Standard ID	LANL Samples						NBL Samples			
	A-1	A-2	B-1	B-2	C-1	C-2	D-1	D-2	E-1	E-2
USIO-91	91.426	91.425	91.434	91.430	91.410	91.411	91.4344	91.4385	91.4253	91.3606
							91.4379	91.4387	91.4314	91.3647
UISO-66	66.330	66.333	66.320	66.295	66.333	66.319	66.3139	66.2786	66.3296	66.2097
							66.3296	66.3023	66.3320	66.3254
UISO-52	52.403	52.411	52.436	52.435	52.416	52.417	52.4478	52.4128	52.4374	52.4695
							52.4114	52.4261	52.4024	52.4367
UISO-38	37.890	37.797	37.910	37.933	37.854	37.847	37.8213	37.8385	37.8588	37.8119
	37.844	37.826					37.8144	37.8261	37.8572	37.8427
UISO-27	26.813	26.659	26.740	26.675	26.811	27.052	26.9594	26.9370	27.0879	27.1561
	26.799	26.647	26.735	26.673	26.810	27.029	26.9426	26.9445	27.0957	27.1526
UISO-17	17.512	17.505	17.491	17.453	17.498	17.473	17.4031	17.4354	17.4353	17.4558
							17.4173	17.4402	17.4145	17.4407
UISO-13	13.108	13.102	13.123	13.087	13.116	13.091	13.1035	13.0923	13.0822	13.0986
							13.0940	13.0900	13.0808	13.0967
UISO-12	11.981	11.912	12.075	12.150	11.921	12.010	11.9093	11.9037	11.9157	11.9180
	11.986	11.902	12.100	12.167	11.921	11.990	11.9067	11.9113	11.9149	11.9045
					11.885					
A1-323-1	10.273	10.204	10.223	10.243	10.314	10.225	10.2120	10.2811	10.2514	10.2040
	10.283	10.225			10.314	10.211	10.2143	10.2572	10.2621	10.2365
	10.308									
A1-324-1	10.207	10.209	10.195	10.200	10.199	10.214	10.1942	10.1867	10.2164	10.1933
							10.2024	10.1986	10.2118	10.2047
A1-324-2	10.197	10.206	10.201	10.199	10.205	10.195	10.1986	10.1931	10.2076	10.1954
							10.2011	10.2011		10.2031
A1-1126-1	3.067	3.066	3.088	3.065	3.074	3.077	3.0659	3.0691	3.0660	3.0658
			3.089	3.067			3.0654	3.0679	3.0673	3.0644

APPENDIX (cont)

Standard ID	LANL Samples						NBL Samples			
	A-1	A-2	B-1	B-2	C-1	C-2	D-1	D-2	E-1	E-2
Al-1126-2	3.061	3.061	3.074	3.074	3.060	3.062	3.0625	3.0659	3.0702	3.0592
							3.0606	3.0666	3.0706	3.0619
Al-1125-1	1.963	1.967	1,963	1.959	1.960	1.962	1.9617	1,9618	1.9609	1,9603
		1.964					1.9621	1.9620	1,9595	1.9615
Al-1125-2	1.973	1.963	1.963	1.965	1.958	1,959	1.9601	1.9598	1.9613	1.9608
	1.973						1.9605	1.9603	1.9606	1.9614
Al-1127-1	0.7279	0.7290	0.7262	0.7265	0.7258	0.7250	0.7255	0.7257	0.7257	0.7264
							0.7240	0.7255	0.7242	0.7257
Al-1127-2	0.7282	0.7280	0.7273	0.7271	0.7257	0.7259	0.7310	0.7255	0.7268	0.7263
							0.7312	0.7252	0.7267	0.7247
Al-408-2	0.721	0.7236	0.7219	0.7226	0.7236	0.7221	0.7228	0.7215	0.7211	0.7210
							0.7228	0.7208	0.7203	0.7204
Al-409	0.7222	0.7194	0.7213	0.7220	0.7205	0.7212	0.7207	0.7198	0.7198	0.7201
							0.7195	0.7193	0.7198	0.7201

Printed in the United States of America
Available from
National Technical Information Service
US Department of Commerce
5285 Port Royal Road
Springfield, VA 22161

Microfiche (A01)

Page Range	NTIS Price Code
001-025	A02
026-050	A03
051-075	A04
076-100	A05
101-125	A06
126-150	A07
151-175	A08
176-200	A09
201-225	A10
226-250	A11
251-275	A12
276-300	A13
301-325	A14
326-350	A15
351-375	A16
376-400	A17
401-425	A18
426-450	A19
451-475	A20
476-500	A21
501-525	A22
526-550	A23
551-575	A24
576-600	A25
601-up*	A99

*Contact NTIS for a price quote.

Los Alamos National Laboratory
Los Alamos,New Mexico 87545